Electronic Supporting Information for

"Controlling the reactions of 1-bromogalactose acetate in methanol using ionic liquids as co-solvents"

Alyssa Gilbert,[a] Ronald S. Haines[a] and Jason B. Harper[a]

[a]*School of Chemistry, University of New South Wales, Sydney, NSW, 2052, Australia*

Synthesis of ionic liquids and precursors

1-Butyl-3-methylimidazolium bromide ([bmim]Br)[1]

1-Methylimidazole (23.0 g, 0.280 mol) and 1-bromobutane (51.2 g, 0.374 mol) were combined and stirred at room temperature under a nitrogen atmosphere for 5 days. Ethyl acetate (30 mL) was added and the mixture was stored at –20 °C overnight. A white solid formed and was triturated with ethyl acetate (5 x 50 mL). The solvent was removed under reduced pressure to give the product as a white solid (59.8 g, 0.273 mol, 96%). m.p. 70-72 °C (lit.[2] 70 °C) ^{1}H NMR (400 MHz, CD_3CN) δ 0.94 (t, J = 7.4 Hz, 3H, CH_2CH_3), 1.28-1.37 (m, 2H, CH_2CH_3), 1.76-1.84 (m, 2H, $CH_2CH_2CH_3$), 3.81 (s, 3H, NCH_3), 4.12 (t, J = 7.4 Hz, 2H, NCH_2CH_2), 7.33-7.36 (m, 2H, NCHCHN), 8.38 (s, 1H, NCHN).

1-Butyl-2,3-dimethylimidazolium chloride ([bm$_2$im]Cl)[3]

1,2-Dimethylimidazole (47.1 g, 0.490 mol) and 1-chlorobutane (54.3 g, 0.587 mol) were combined and stirred at 75 °C under a nitrogen atmosphere for 7 days. During this time a white solid formed. The solid was dissolved in acetonitrile (100 mL) and the solution was stirred at 75 °C under a nitrogen atmosphere for a further 28 days. The acetonitrile was removed under reduced pressure and the resultant solid was recrystallised from a 3:2 mixture of acetonitrile and ethyl acetate to give the product as a white solid (76.8 g, 0.406 mol, 83%). m.p. 92-95 °C (lit.[4] 93 °C). ^{1}H NMR (400 MHz, CD_3CN). δ 0.94 (t, J = 7.4 Hz, 3H, CH_2CH_3), 1.30-1.39 (m, 2H, CH_2CH_3), 1.70-1.77 (m, 2H, $CH_2CH_2CH_3$), 2.51 (s, 3H, $NC(CH_3)NCH_3$), 3.72 (s, 1H, NCH_3), 4.05 (t, J = 7.4 Hz, 2H, NCH_2CH_2), 7.34-7.35 (m, 2H, NCHCHN).

1-Butyl-1-methylpyrrolidinium bromide ([bmpyr]Br)[5]

1-Methylpyrrolidine (31.1 g, 0.365 mol) and 1-bromobutane (63.2 g, 0.461 mol) were combined and stirred at room temperature under a nitrogen atmosphere for 22 hours. During this time, a white solid formed. Acetonitrile (80 mL) was added to dissolve the solid and the solution was mixed for a further 24 hours at room temperature under a nitrogen atmosphere. The acetonitrile was removed under reduced pressure and a white solid formed. The solid was

triturated with ethyl acetate (3 x 50 mL) and the solvent removed under reduced pressure. The solid was recrystallised from a 1:1 mixture of acetonitrile/ethyl acetate and dried under reduced pressure to give the product as a white crystalline solid (65.3 g, 0.294 mol, 81%). m.p. 204-205 °C. (lit.[6] 216-217 °C). ^{1}H NMR (400 MHz, CD_3CN) δ 0.97 (t, J = 7.4 Hz, 3H, CH_3CH_2), 1.33-1.42 (m, 2H, CH_2CH_3), 1.68-1.76 (m, 2H, $CH_2CH_2CH_3$), 2.15-2.16 (m, 4H, $NCH_2CH_2CH_2$), 2.98 (s, 3H, NCH_3), 3.26-3.31 (m, 2H, NCH_2CH_2), 3.45-3.46 (m, 4H, CH_2NCH_2).

1-Butyl-3-methylimidazolium chloride ([bmim]Cl)[3]

1-Methylimidazole (33.0 g, 0.402 mol) and 1-chlorobutane (32.8 g, 0.315 mol) were combined and heated to 100 °C for 45 minutes under microwave irradiation. Ethyl acetate (50 mL) was added, and the mixture stirred at room temperature for 15 mins. During this time, a white solid formed. The solvent was decanted and the solid was triturated with ethyl acetate (6 x 50 mL). The solid was dried under reduced pressure to give the product as a white solid (45.2 g, 0.259 mol, 82%). m.p. 65-67 °C (lit.[7] 65 °C). ^{1}H NMR (400 MHz, CD_3CN) δ 0.93 (t, J = 7.4 Hz, 3H, CH_2CH_3), 1.27-1.37 (m, 2H, CH_2CH_3), 1.78-1.86 (m, 2H, $CH_2CH_2CH_3$), 3.88 (s, 3H, NCH_3), 4.20 (t, J = 7.4 Hz, 2H, NCH_2CH_2), 7.43-7.46 (m, 2H, NCHCHN), 9.52 (s, 1H, NCHN).

1-Butyl-3-methylimidazolium *bis*(trifluoromethanesulfonyl)imide ([bmim][$N(SO_2CF_3)_2$], **3**)[8]

1-Butyl-3-methylimidazolium bromide (106 g, 0.486 mol) in water (250 mL) and lithium *bis*(trifluoromethanesulfonyl)imide (158 g, 0.551 mol) in water (200 mL) were combined and the resultant mixture was stirred at room temperature for 18 hours. During this time, two immiscible layers formed. The aqueous layer was extracted with dichloromethane (3 x 150 mL) and the organic layers were combined and washed with water (10 x 200 mL). The organic layer was dried with magnesium sulfate and the solvent was removed under reduced pressure to give the product as a colourless liquid (184 g, 0.439 mol, 90%). ^{1}H NMR (400 MHz, CD_3CN) δ 0.94 (t, J = 7.4 Hz, 3H, CH_2CH_3), 1.28-1.37 (m, 2H, CH_2CH_3), 1.76-1.84 (m, 2H, $CH_2CH_2CH_3$), 3.81 (s, 3H, NCH_3), 4.11 (t, J = 7.4 Hz, 2H, NCH_2CH_2), 7.32-7.36 (m, 2H, NCHCHN), 8.38 (s, 1H, NCHN).

1-Butyl-2,3-dimethylimidazolium *bis*(trifluoromethanesulfonyl)imide ([bm_2im][$N(SO_2CF_3)_2$], **4**)[3]

1-Butyl-2,3-dimethylimidazolium chloride (30.3 g, 0.161 mol) dissolved in water (40 mL) and lithium *bis*(trifluoromethanesulfonyl)imide (51.0 g, 0.178 mol) dissolved in water (60 mL) were combined and stirred at room temperature for 24 hours. During this time, two immiscible layers formed. The aqueous layer was extracted with dichloromethane (3 x 25 mL), the organic layers were combined and washed with water (10 x 100 mL). The organic layer was dried with magnesium sulfate and the solvent removed under reduced pressure to give the product **4** as a pale yellow liquid (58.6 g, 0.135 mol, 84%). ^{1}H NMR (400 MHz, CD_3CN). δ 0.94 (t, J = 7.4 Hz, 3H, CH_2CH_3), 1.30-1.39 (m, 2H, CH_2CH_3), 1.70-1.77 (m, 2H, $CH_2CH_2CH_3$), 2.49 (s, 3H, $NC(CH_3)NCH_3$), 3.68 (s, 1H, NCH_3), 4.02 (t, J = 7.4 Hz, 2H, NCH_2CH_2), 7.23-7.25 (m, 2H, NCHCHN).

1-Butyl-1-methylpyrrolidinium *bis*(trifluoromethanesulfonyl)imide ([bmpyr][$N(SO_2CF_3)_2$], **5**)[8]

1-Butyl-1-methylpyrrolidinium bromide (35.2 g, 0.158 mol) and lithium *bis*(trifluoromethanesulfonyl)imide (49.9 g, 0.174 mol) were dissolved in water (150 mL) and the resultant mixture was stirred at room temperature for 20 hours. During this time, two immiscible layers formed. The aqueous layer was extracted with dichloromethane (3 x 100 mL) and the organic layers were combined and washed with water (10 x 100 mL). The organic layer was dried with magnesium sulfate and the solvent was removed under reduced pressure to give the product **5** as a colourless liquid (52.0 g, 0.123 mol, 78%). ^{1}H NMR (400 MHz, CD_3CN) δ 0.96 (t, J = 7.4 Hz, 3H, CH_3CH_2), 1.34-1.41 (m, 2H, CH_2CH_3), 1.67-1.75 (m, 2H, $CH_2CH_2CH_3$), 2.14-2.15 (m, 4H, $NCH_2CH_2CH_2$), 2.93 (s, 3H, NCH_3), 3.19-3.23 (m, 2H, NCH_2CH_2), 3.39-3.40 (m, 4H, CH_2NCH_2).

Methyltrioctylammonium *bis*(trifluoromethanesulfonyl)imide ([mtoa][$N(SO_2CF_3)_2$], **6**)[9]

A combination of methyltrioctylammonium bromide (14.8 g, 0.033 mol) dissolved in acetone (50 mL) and lithium *bis*(trifluoromethanesulfonyl)imide (10.4 g, 0.036 mol) dissolved in water (50 mL) was stirred at room temperature for 20 hours. The acetone was removed under reduced pressure, leaving two immiscible layers. The aqueous layer was extracted with dichloromethane (3 x 50 mL). The organic layers were combined, washed with water (10 x 100 mL) and dried using magnesium sulfate. The solvent was removed under reduced pressure to give the product **6** as a yellow, viscous liquid (19.3 g, 0.030 mol, 90%). ^{1}H NMR (400 MHz, CD_3CN) δ 0.90 (t, J = 7.4 Hz, 9H, CH_3CH_2), 1.30-1.33 (m, 30H, $(CH_2)_5CH_3$), 1.61-1.65 (m, 6H, NCH_2CH_2), 2.85 (s, 3H, NCH_3), 3.07-3.12 (m, 6H, NCH_2CH_2).

1-Butyl-3-methylimidazolium hexafluorophosphate ([bmim][PF_6], **7**)[3]

1-Butyl-3-methylimidazolium bromide (39.5 g, 0.180 mol) dissolved in water (50 mL) and potassium hexafluorophosphate (36.5 g, 0.198 mol) dissolved in water (100 mL) were combined and the resultant mixture was stirred at room temperature for 20 hours, during which time two immiscible layers formed. The aqueous layer was extracted with dichloromethane (3 x 50 mL), the organic layers were combined and washed with water (10 x 100 mL). The organic layer was dried with magnesium sulfate and the solvent removed was under reduced pressure to give the product **7** as a colourless liquid (37.1 g, 0.131 mol, 73%). ^{1}H NMR (400 MHz, CD_3CN) δ 0.94 (t, J = 7.4 Hz, 3H, CH_2CH_3), 1.28-1.37 (m, 2H, CH_2CH_3), 1.78-1.85 (m, 2H, $CH_2CH_2CH_3$), 3.85 (s, 3H, NCH_3), 4.17 (t, J = 7.4 Hz, 2H, NCH_2CH_2), 7.38-7.42 (m, 2H, NCHCHN), 8.93 (s, 1H, NCHN).

1-Butyl-3-methylimidazolium tetrafluoroborate ([bmim][BF_4], **8**)[8]

1-Butyl-3-methylimidazolium chloride (45.2 g, 0.259 mol) and sodium tetrafluoroborate (32.2 g, 0.293 mol) were each dissolved in dichloromethane (100 mL total) and the resultant mixture was stirred at room temperature for 16 hours. Sodium chloride formed as a white precipitate and was collected through filtration and discarded. The solvent was removed under reduced pressure and dichloromethane (100 mL) was added. The solution was stored at –20 °C

overnight to further assist in precipitation of any remaining sodium chloride. The precipitate was again filtered and discarded and the filtrate again stored at –20 °C overnight. This process was repeated 8 times to ensure complete removal of sodium chloride. Ion chromatography confirmed the chloride content as <20 ppm. The solvent was removed under reduced pressure to give the product **8** as a colourless liquid (31.7 g, 0.140 mol, 54%). ^{1}H NMR (400 MHz, CD_3CN) δ 0.94 (t, J = 7.4 Hz, 3H, CH_2CH_3), 1.28-1.37 (m, 2H, CH_2CH_3), 1.76-1.84 (m, 2H, $CH_2CH_2CH_3$), 3.82 (s, 3H, NCH_3), 4.12 (t, J = 7.4 Hz, 2H, NCH_2CH_2), 7.33-7.36 (m, 2H, NCHCHN), 8.41 (s, 1H, NCHN).

1-Butyl-3-methylimidazolium tricyanomethanide ([bmim][$C(CN)_3$], **9**)[10]

1-Butyl-3-methylimidazolium bromide (26.9 g, 0.123 mol) and sodium tricyanomethanide (15.4 g, 0.136 mol) were each dissolved in water (100 mL total) and the resulting mixture was stirred at room temperature for 20 hours. Two immiscible layers formed. The aqueous layer was extracted with dichloromethane (3 x 50 mL). The combined organic layers were washed with water (8 x 100 mL) and dried with magnesium sulfate. The solvent was removed under reduced pressure to give the product **9** as a pale orange liquid (20.1 g, 0.088 mol, 71%). ^{1}H NMR (400 MHz, CD_3CN) δ 0.94 (t, J = 7.4 Hz, 3H, CH_2CH_3), 1.28-1.38 (m, 2H, CH_2CH_3), 1.77-1.84 (m, 2H, $CH_2CH_2CH_3$), 3.82 (s, 3H, NCH_3), 4.12 (t, J = 7.4 Hz, 2H, NCH_2CH_2), 7.33-7.37 (m, 2H, NCHCHN), 8.40 (s, 1H, NCHN).

Experimental details for kinetic analyses

All kinetic experiments were performed in triplicate using either a Bruker Avance III 400, Bruker Avance III 500 or Bruker Avance III 600 sprectrometer with either a TBI or BBFO probe. Results were shown to be reproducible between spectrometers.

Stock solutions were prepared containing the electrophile **1** (*ca.* 0.005 mol L^{-1}), triethylamine (*ca.* 0.02 mol L^{-1}), and the desired solvent mixture of methanol and one of the ionic liquids **3-9**. An aliquot (0.5 mL) of each stock solution was placed in an NMR tube. Each stock solution was measured in triplicate.

All cases were monitored using ^{1}H NMR spectroscopy by following the depletion of the signal representing the H1 proton of the electrophile **1** at *ca.* 6.5 ppm to more than 95% completion. Mole fraction dependence studies were performed at 42.0 °C; temperature dependence studies were performed over a range from 33.4-58.2 °C. Reactions were monitored *in situ* for χ_{IL} = 0.01-0.50 for ionic liquids **3-5**, χ_{IL} = 0.01-0.32 for ionic liquid **6**, and for all solvent compositions of ionic liquids **7-9**. For the solvent compositions not already mentioned, the reaction mixtures were placed in a water bath set to the desired temperature and NMR spectra taken at time points throughout the reaction progression.

NMR spectra obtained for kinetic analyses were processed using MestReNova 10.1 software. The first order rate constant was obtained by taking the natural logarithm of the integration of the signal at *ca.* 6.5 ppm over time.

Where applicable, the enthalpy and entropy of activation were calculated using the Eyring equation (Equation 1).[11]

$$ln\left(\frac{k_1 h}{k_B T}\right) = \frac{\Delta S^{\ddagger}}{R} - \frac{\Delta H^{\ddagger}}{RT} \qquad (1)$$

Nucleophile dependence plot

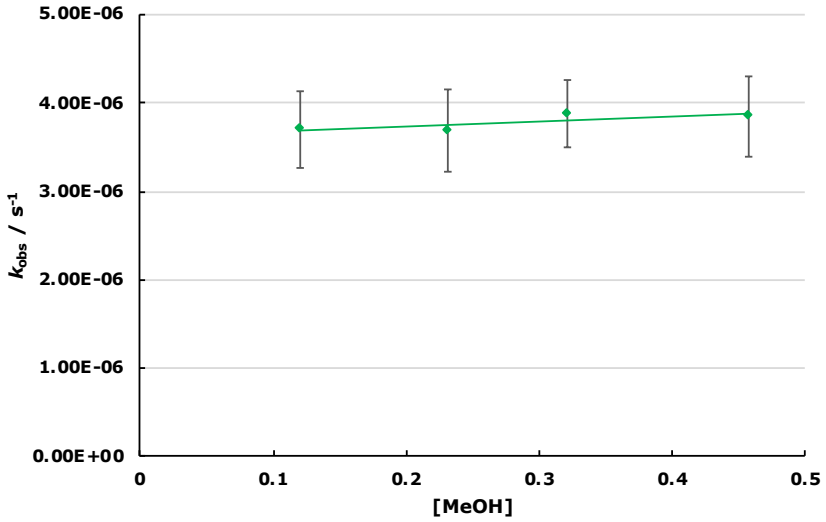

Figure S1. The nucleophile dependence plot for the reaction between the galactose **1** and methanol in acetonitrile, showing the lack of dependence on the concentration of methanol, indicating the unimolecular substitution mechanism of the reaction (slope = (5.23 ± 8.97) x 10^{-7} s^{-1}).

Mole Fraction dependence plots for ionic liquids 4-9

All mole fraction dependence plots below contain data for each ionic liquid **4-9** combined with the mole fraction dependence data for [bmim][$N(SO_2CF_3)_2$] **3** for comparison.

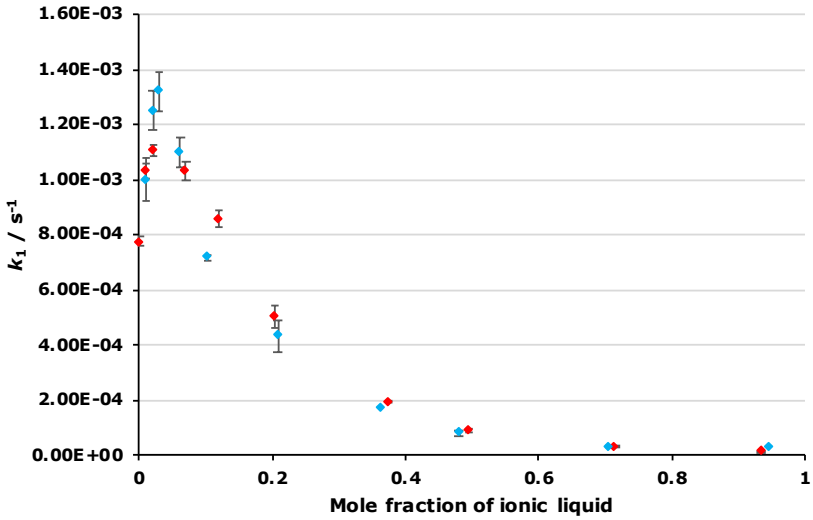

Figure S2. The dependence of the unimolecular rate constant (k_1) of the solvolysis of acetobromogalactose **1** on the mole fraction of [bm_2im][$N(SO_2CF_3)_2$] **4** (♦) or [bmim][$N(SO_2CF_3)_2$] **3** (♦) in methanol. Uncertainties reported are the standard deviation of triplicate measurements; some uncertainties fall within the size of the markers used.

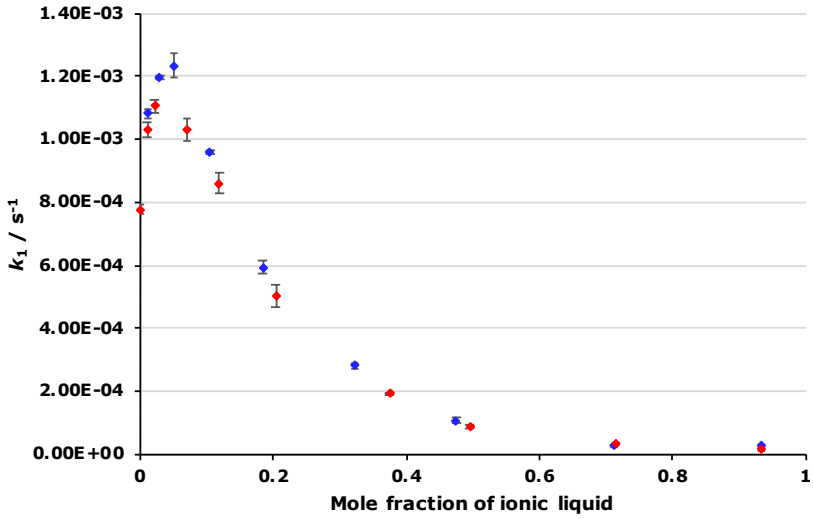

Figure S3. The dependence of the unimolecular rate constant (k_1) of the solvolysis of acetobromogalactose **1** on the mole fraction of [bmpyr][$N(SO_2CF_3)_2$] **5** (♦) or [bmim][$N(SO_2CF_3)_2$] **3** (♦) in methanol. Uncertainties reported are the standard deviation of triplicate measurements; some uncertainties fall within the size of the markers used.

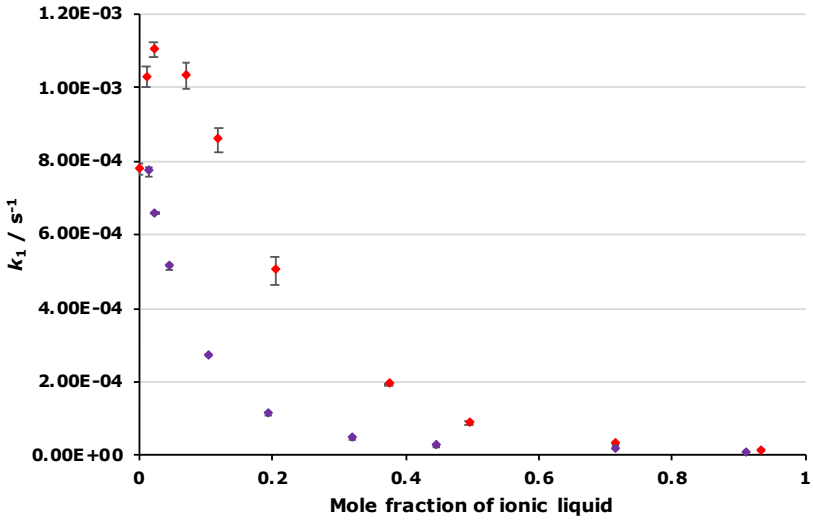

Figure S4. The dependence of the unimolecular rate constant (k_1) of the solvolysis of acetobromogalactose **1** on the mole fraction of [mtoa][$N(SO_2CF_3)_2$] **6** (♦) or [bmim][$N(SO_2CF_3)_2$] **3** (♦) in methanol. Uncertainties reported are the standard deviation of triplicate measurements; some uncertainties fall within the size of the markers used.

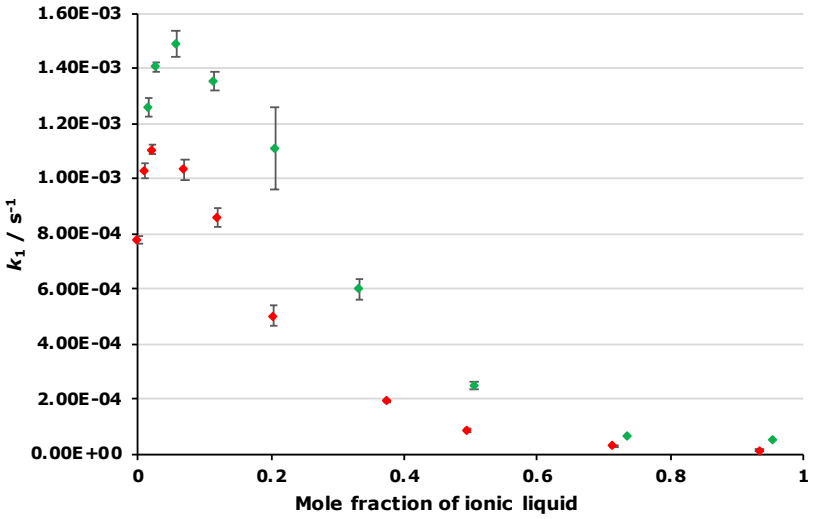

Figure S5. The dependence of the unimolecular rate constant (k_1) of the solvolysis of acetobromogalactose **1** on the mole fraction of [bmim][PF_6] **7** (♦) or [bmim][$N(SO_2CF_3)_2$] **3** (♦) in methanol. Uncertainties reported are the standard deviation of triplicate measurements; some uncertainties fall within the size of the markers used.

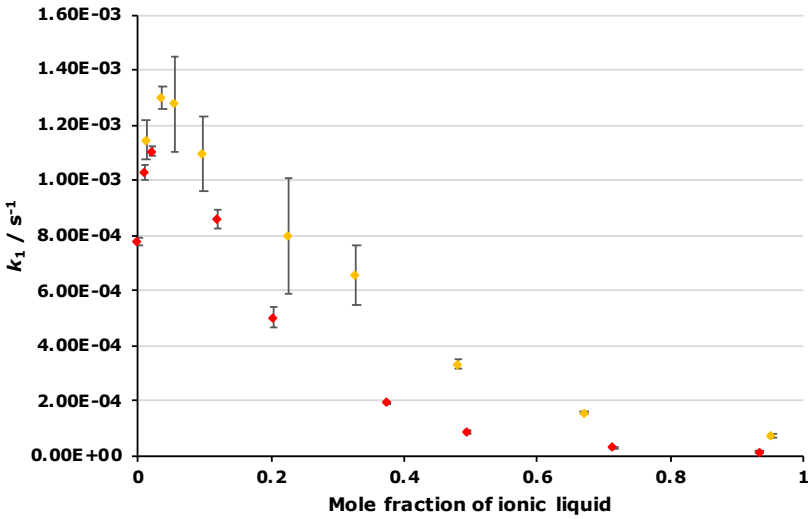

Figure S6. The dependence of the unimolecular rate constant (k_1) of the solvolysis of acetobromogalactose **1** on the mole fraction of [bmim][BF_4] **8** (♦) or [bmim][$N(SO_2CF_3)_2$] **3** (♦) in methanol. Uncertainties reported are the standard deviation of triplicate measurements; some uncertainties fall within the size of the markers used.

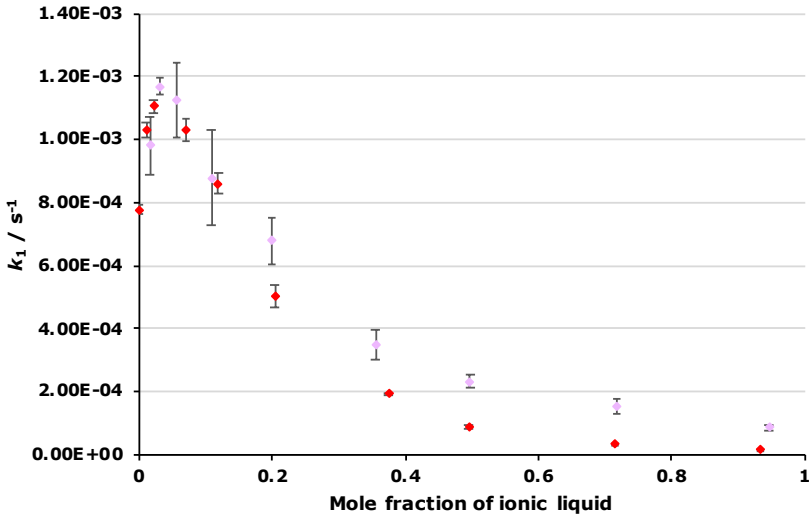

Figure S7. The dependence of the unimolecular rate constant (k_1) of the solvolysis of acetobromogalactose **1** on the mole fraction of [bmim][$C(CN)_3$] **9** (♦) or [bmim][$N(SO_2CF_3)_2$] **3** (♦) in methanol. Uncertainties reported are the standard deviation of triplicate measurements; some uncertainties fall within the size of the markers used.

Eyring plot

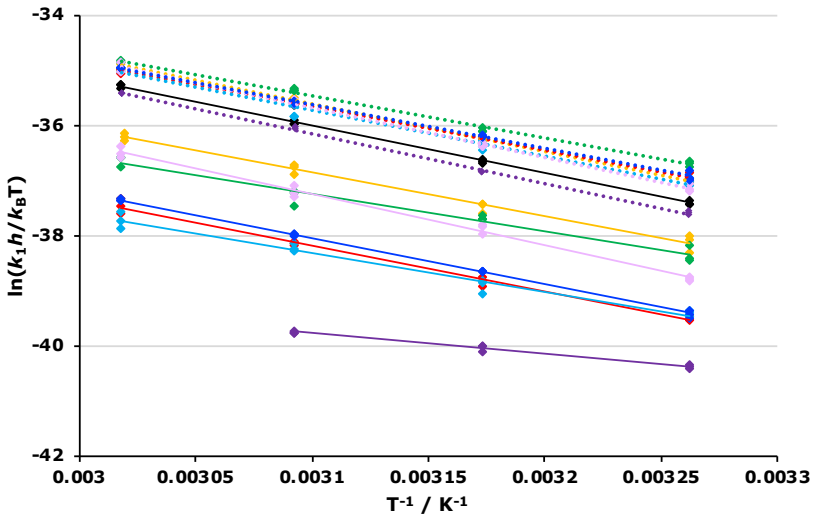

Figure S8. The Eyring plot from which the activation parameters were determined for the solvolysis of the galactose **1** in methanol only (♦) or mixtures of methanol and one of the ionic liquids [bmim][$N(SO_2CF_3)_2$] **3** (♦), [bm_2im][$N(SO_2CF_3)_2$] **4** (♦), [bmpyr][$N(SO_2CF_3)_2$] **5** (♦), [mtoa][$N(SO_2CF_3)_2$] **6** (♦), [bmim][PF_6] **7** (♦), [bmim][BF_4] **8** (♦) or [bmim][$C(CN)_3$] **9** (♦) at χ *ca.* 0.02 (denoted by dotted lines) or χ *ca.* 0.50 (denoted by solid lines).

Natural logarithm of k_1 *vs* Kamlet–Taft solvent parameter plots

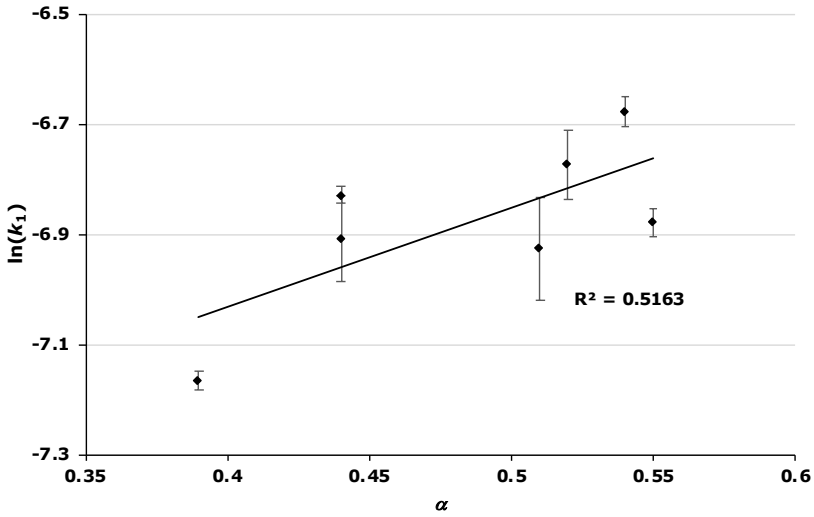

Figure S9. The relationship between the natural logarithm of the rate constant and the α Kamlet–Taft parameter for the solvolysis of the galactose **1** for each of the ionic liquids **3-9** at χ *ca.* 0.01. Uncertainties are calculated from the standard deviation of triplicate measurements and transformed on calculating the natural logarithm.

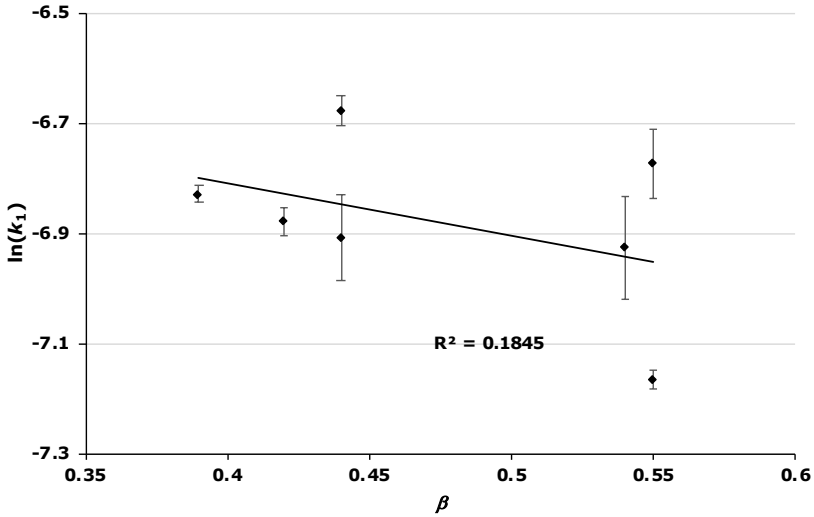

Figure S10. The relationship between the natural logarithm of the rate constant and the β Kamlet–Taft parameter for the solvolysis of the galactose **1** for each of the ionic liquids **3-9** at χ *ca.* 0.01. Uncertainties are calculated from the standard deviation of triplicate measurements and transformed on calculating the natural logarithm.

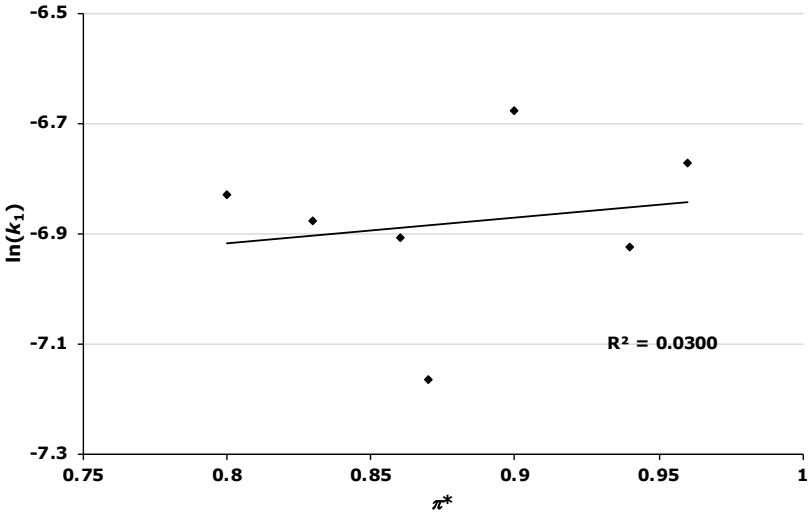

Figure S11. The relationship between the natural logarithm of the rate constant and the π^* Kamlet–Taft parameter for the solvolysis of the galactose **1** for each of the ionic liquids **3-9** at χ *ca.* 0.01. Uncertainties are calculated from the standard deviation of triplicate measurements and transformed on calculating the natural logarithm.

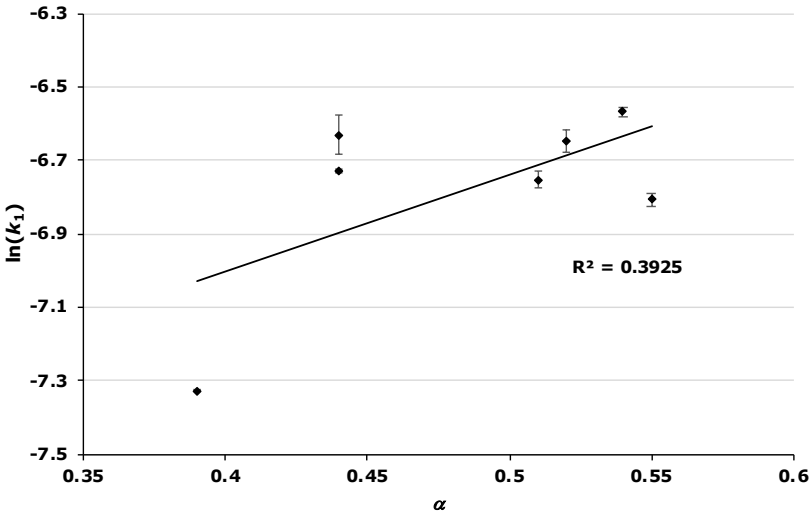

Figure S12. The relationship between the natural logarithm of the rate constant and the α Kamlet–Taft parameter for the solvolysis of the galactose **1** for each of the ionic liquids **3-9** at χ *ca.* 0.02. Uncertainties are calculated from the standard deviation of triplicate measurements and transformed on calculating the natural logarithm.

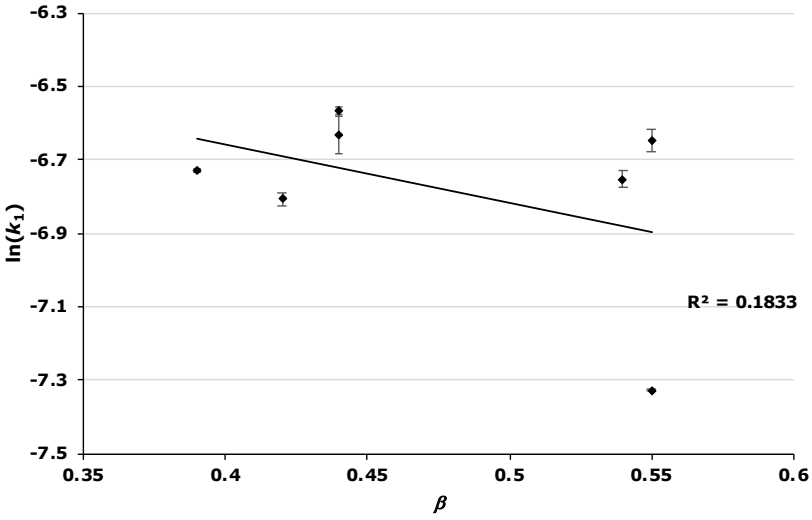

Figure S13. The relationship between the natural logarithm of the rate constant and the β Kamlet–Taft parameter for the solvolysis of the galactose **1** for each of the ionic liquids **3-9** at χ *ca.* 0.02. Uncertainties are calculated from the standard deviation of triplicate measurements and transformed on calculating the natural logarithm.

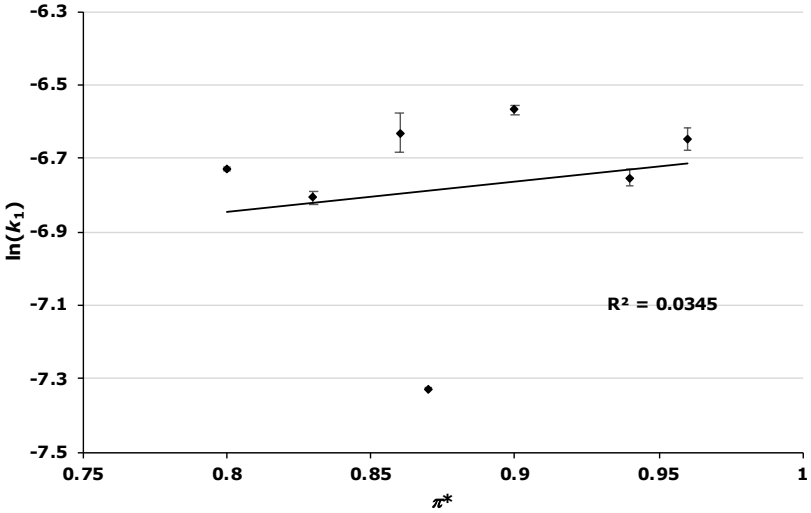

Figure S14. The relationship between the natural logarithm of the rate constant and the π^* Kamlet–Taft parameter for the solvolysis of the galactose **1** for each of the ionic liquids **3-9** at χ *ca.* 0.02. Uncertainties are calculated from the standard deviation of triplicate measurements and transformed on calculating the natural logarithm.

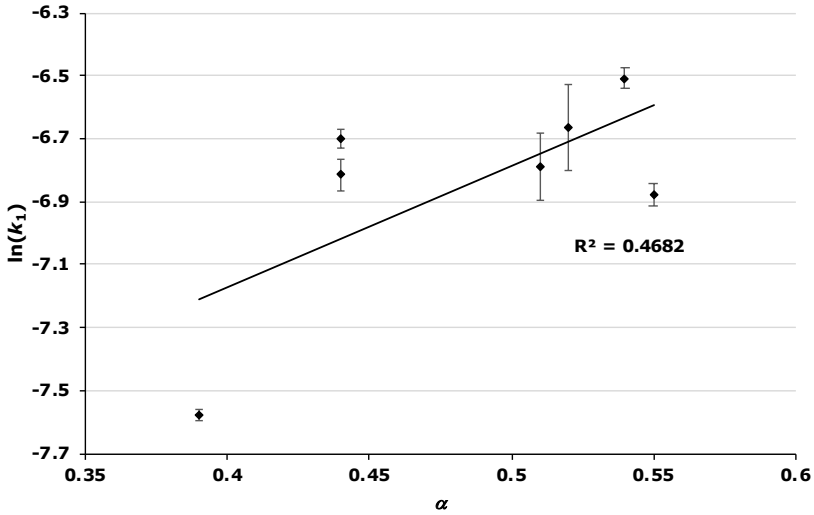

Figure S15. The relationship between the natural logarithm of the rate constant and the α Kamlet–Taft parameter for the solvolysis of the galactose **1** for each of the ionic liquids **3-9** at χ *ca.* 0.05. Uncertainties are calculated from the standard deviation of triplicate measurements and transformed on calculating the natural logarithm.

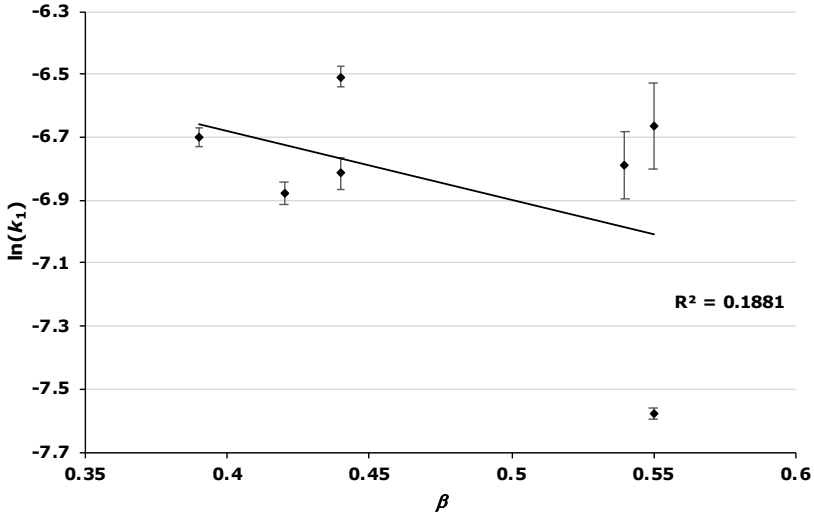

Figure S16. The relationship between the natural logarithm of the rate constant and the β Kamlet–Taft parameter for the solvolysis of the galactose **1** for each of the ionic liquids **3-9** at χ *ca.* 0.05. Uncertainties are calculated from the standard deviation of triplicate measurements and transformed on calculating the natural logarithm.

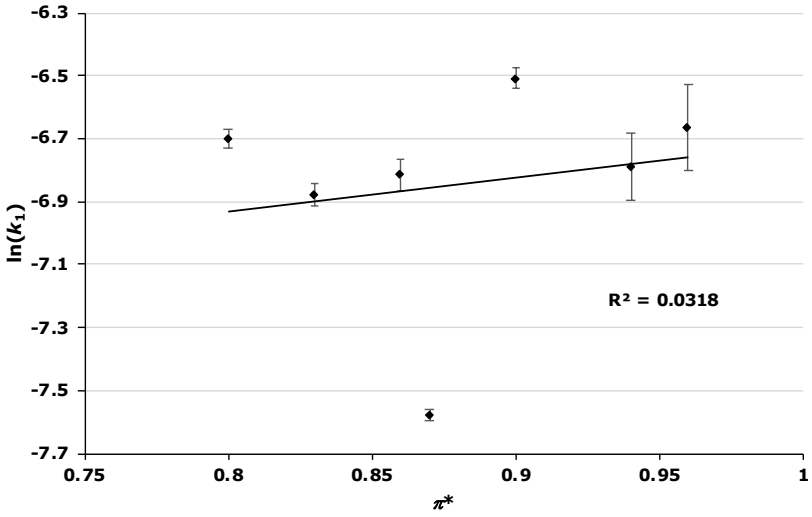

Figure S17. The relationship between the natural logarithm of the rate constant and the π^* Kamlet–Taft parameter for the solvolysis of the galactose **1** for each of the ionic liquids **3-9** at χ *ca.* 0.05. Uncertainties are calculated from the standard deviation of triplicate measurements and transformed on calculating the natural logarithm.

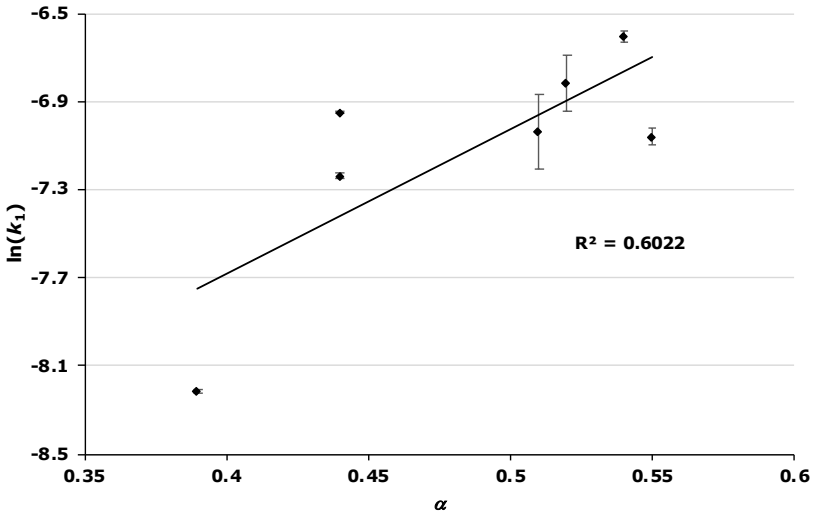

Figure S18. The relationship between the natural logarithm of the rate constant and the α Kamlet–Taft parameter for the solvolysis of the galactose **1** for each of the ionic liquids **3-9** at χ *ca.* 0.10. Uncertainties are calculated from the standard deviation of triplicate measurements and transformed on calculating the natural logarithm.

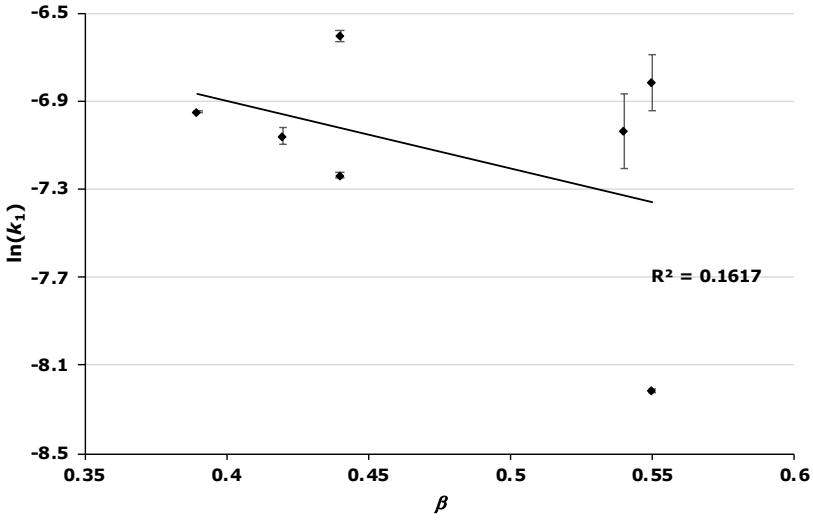

Figure S19. The relationship between the natural logarithm of the rate constant and the β Kamlet–Taft parameter for the solvolysis of the galactose **1** for each of the ionic liquids **3-9** at χ *ca.* 0.10. Uncertainties are calculated from the standard deviation of triplicate measurements and transformed on calculating the natural logarithm.

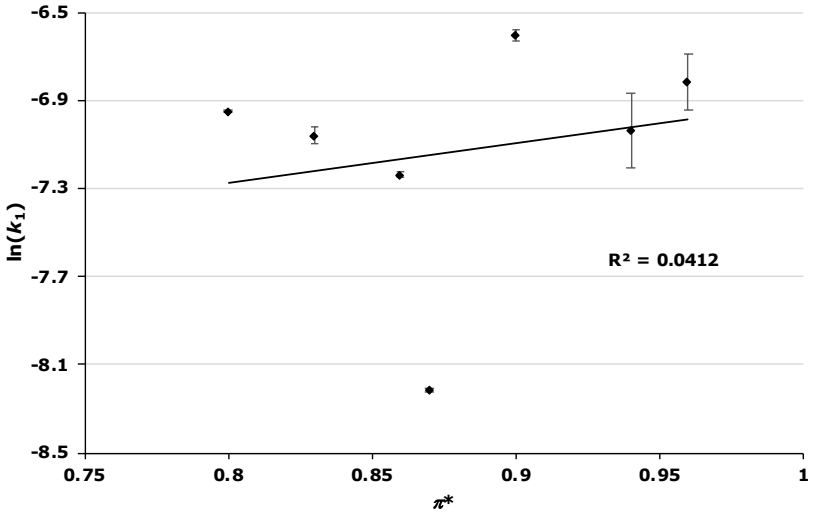

Figure S20. The relationship between the natural logarithm of the rate constant and the π^* Kamlet–Taft parameter for the solvolysis of the galactose **1** for each of the ionic liquids **3-9** at χ *ca.* 0.10. Uncertainties are calculated from the standard deviation of triplicate measurements and transformed on calculating the natural logarithm.

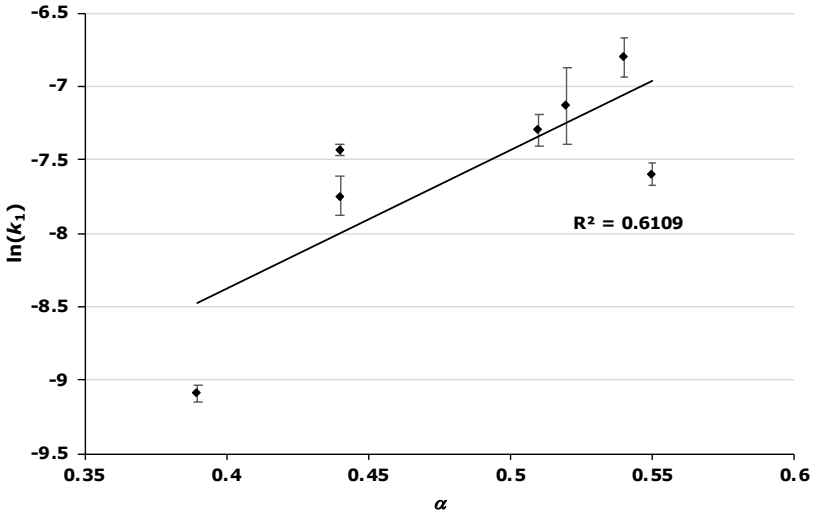

Figure S21. The relationship between the natural logarithm of the rate constant and the α Kamlet–Taft parameter for the solvolysis of the galactose **1** for each of the ionic liquids **3-9** at χ *ca.* 0.20. Uncertainties are calculated from the standard deviation of triplicate measurements and transformed on calculating the natural logarithm.

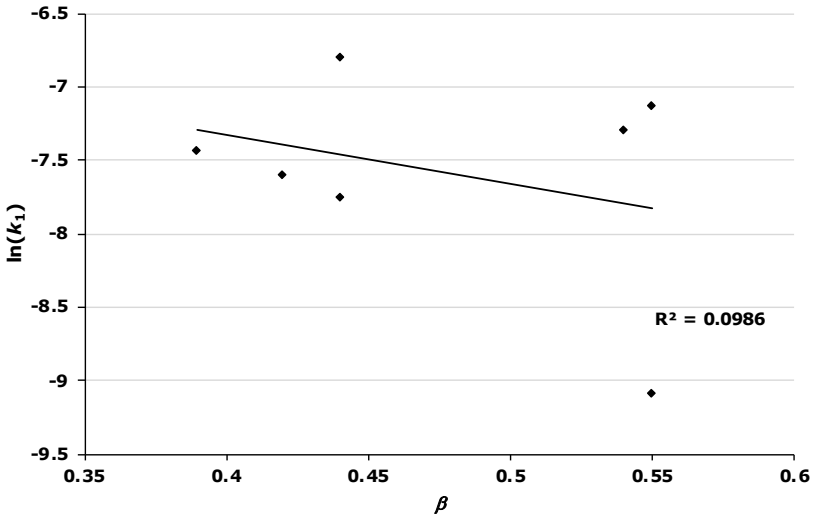

Figure S22. The relationship between the natural logarithm of the rate constant and the β Kamlet–Taft parameter for the solvolysis of the galactose **1** for each of the ionic liquids **3-9** at χ *ca.* 0.20. Uncertainties are calculated from the standard deviation of triplicate measurements and transformed on calculating the natural logarithm.

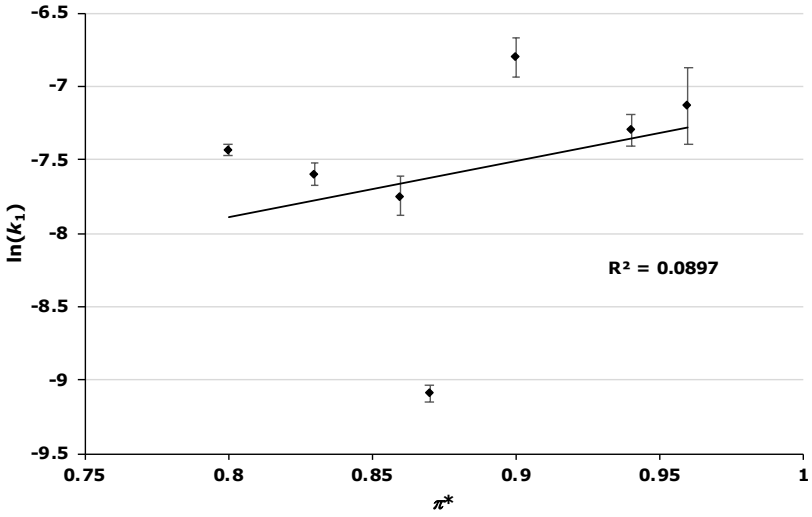

Figure S23. The relationship between the natural logarithm of the rate constant and the π^* Kamlet–Taft parameter for the solvolysis of the galactose **1** for each of the ionic liquids **3-9** at χ *ca.* 0.20. Uncertainties are calculated from the standard deviation of triplicate measurements and transformed on calculating the natural logarithm.

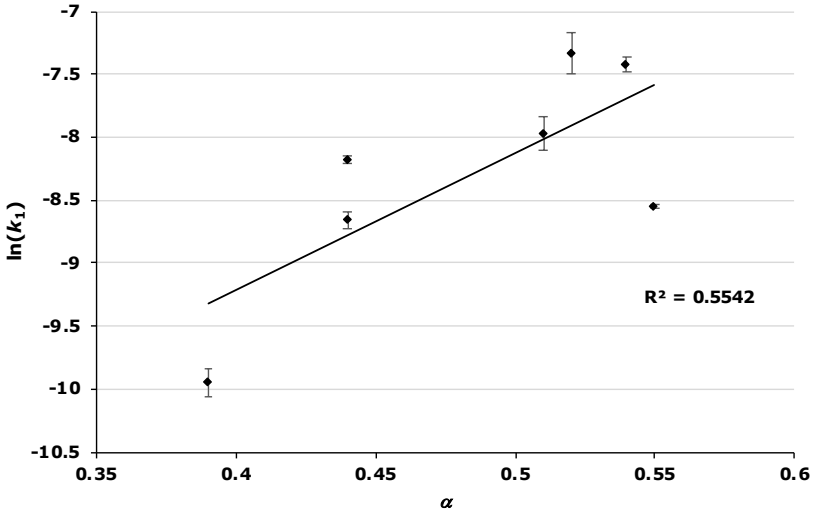

Figure S24. The relationship between the natural logarithm of the rate constant and the α Kamlet–Taft parameter for the solvolysis of the galactose **1** for each of the ionic liquids **3-9** at χ *ca.* 0.35. Uncertainties are calculated from the standard deviation of triplicate measurements and transformed on calculating the natural logarithm.

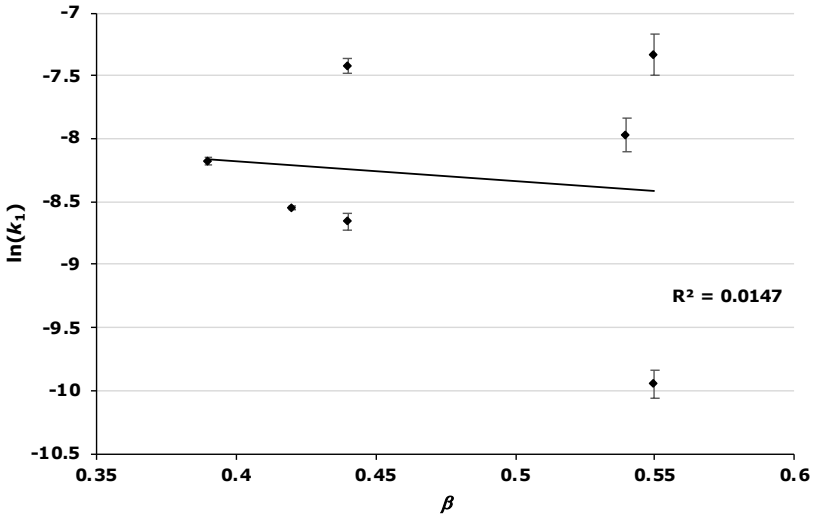

Figure S25. The relationship between the natural logarithm of the rate constant and the β Kamlet–Taft parameter for the solvolysis of the galactose **1** for each of the ionic liquids **3-9** at χ *ca.* 0.35. Uncertainties are calculated from the standard deviation of triplicate measurements and transformed on calculating the natural logarithm.

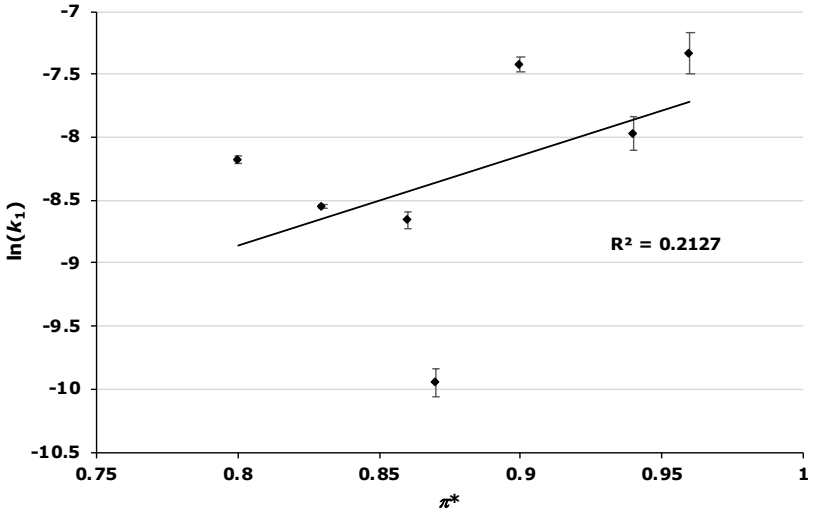

Figure S26. The relationship between the natural logarithm of the rate constant and the π^* Kamlet–Taft parameter for the solvolysis of the galactose **1** for each of the ionic liquids **3-9** at χ *ca.* 0.35. Uncertainties are calculated from the standard deviation of triplicate measurements and transformed on calculating the natural logarithm.

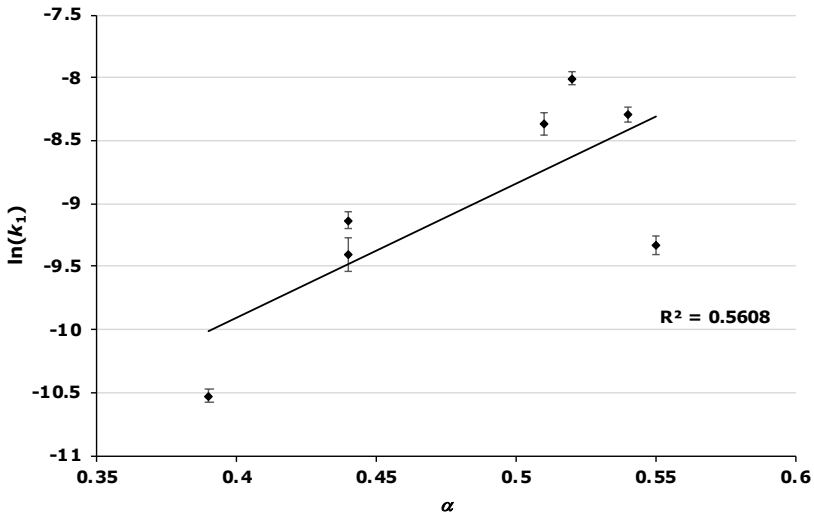

Figure S27. The relationship between the natural logarithm of the rate constant and the α Kamlet–Taft parameter for the solvolysis of the galactose **1** for each of the ionic liquids **3-9** at χ *ca.* 0.50. Uncertainties are calculated from the standard deviation of triplicate measurements and transformed on calculating the natural logarithm.

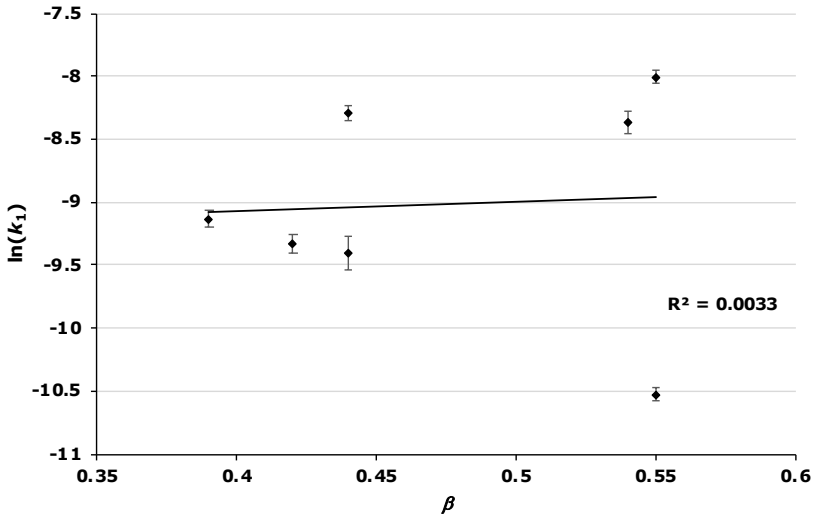

Figure S28. The relationship between the natural logarithm of the rate constant and the β Kamlet–Taft parameter for the solvolysis of the galactose **1** for each of the ionic liquids **3-9** at χ *ca.* 0.50. Uncertainties are calculated from the standard deviation of triplicate measurements and transformed on calculating the natural logarithm.

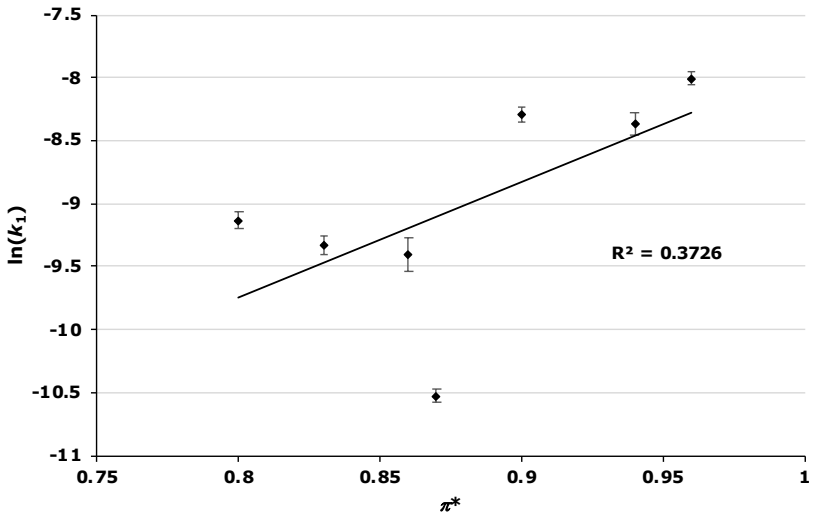

Figure S29. The relationship between the natural logarithm of the rate constant and the π^* Kamlet–Taft parameter for the solvolysis of the galactose **1** for each of the ionic liquids **3-9** at χ *ca.* 0.50. Uncertainties are calculated from the standard deviation of triplicate measurements and transformed on calculating the natural logarithm.

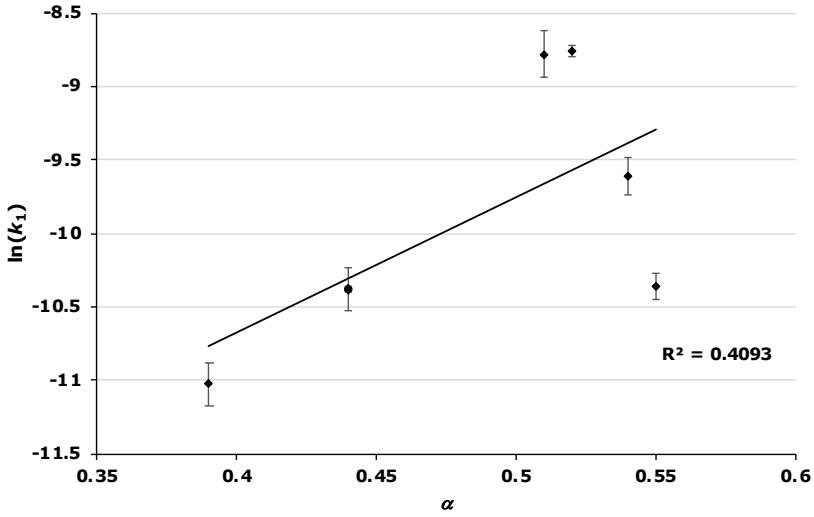

Figure S30. The relationship between the natural logarithm of the rate constant and the α Kamlet–Taft parameter for the solvolysis of the galactose **1** for each of the ionic liquids **3-9** at χ *ca.* 0.73. Uncertainties are calculated from the standard deviation of triplicate measurements and transformed on calculating the natural logarithm.

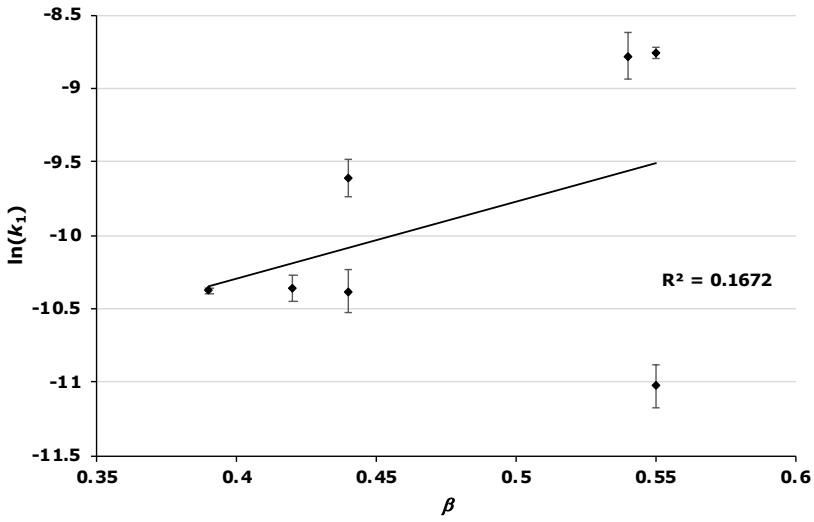

Figure S31. The relationship between the natural logarithm of the rate constant and the β Kamlet–Taft parameter for the solvolysis of the galactose **1** for each of the ionic liquids **3-9** at χ *ca.* 0.73. Uncertainties are calculated from the standard deviation of triplicate measurements and transformed on calculating the natural logarithm.

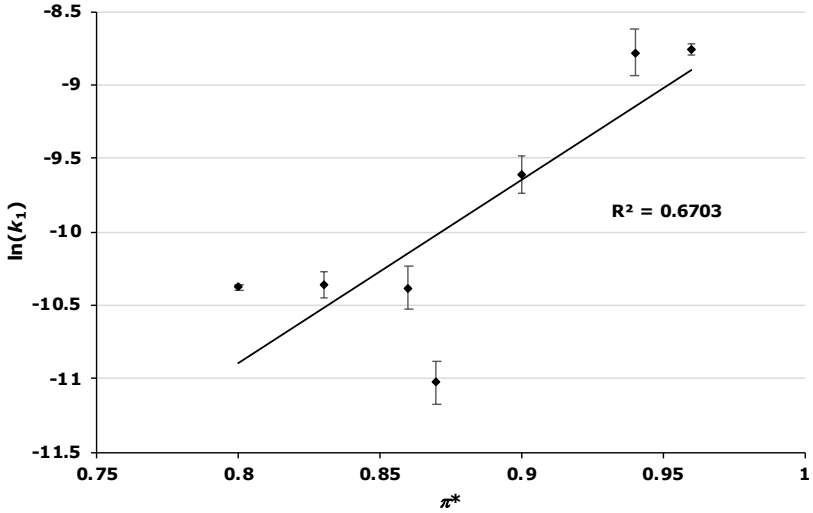

Figure S32. The relationship between the natural logarithm of the rate constant and the π^*Kamlet–Taft parameter for the solvolysis of the galactose **1** for each of the ionic liquids **3-9** at χ *ca.* 0.73. Uncertainties are calculated from the standard deviation of triplicate measurements and transformed on calculating the natural logarithm.

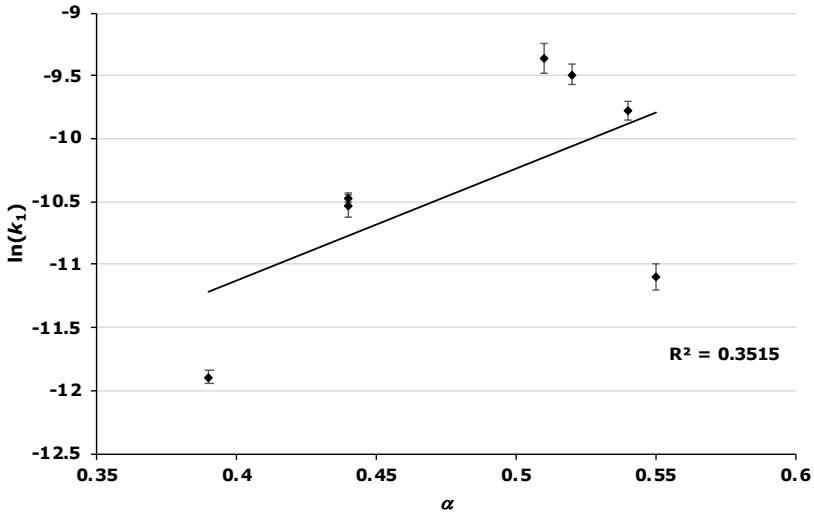

Figure S33. The relationship between the natural logarithm of the rate constant and the α Kamlet–Taft parameter for the solvolysis of the galactose **1** for each of the ionic liquids **3-9** at χ *ca.* 0.95. Uncertainties are calculated from the standard deviation of triplicate measurements and transformed on calculating the natural logarithm.

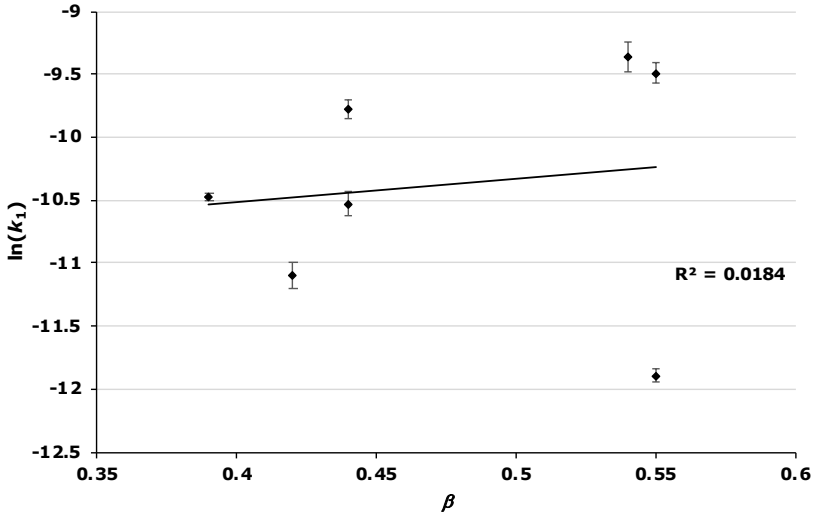

Figure S34. The relationship between the natural logarithm of the rate constant and the β Kamlet–Taft parameter for the solvolysis of the galactose **1** for each of the ionic liquids **3-9** at χ *ca.* 0.95. Uncertainties are calculated from the standard deviation of triplicate measurements and transformed on calculating the natural logarithm.

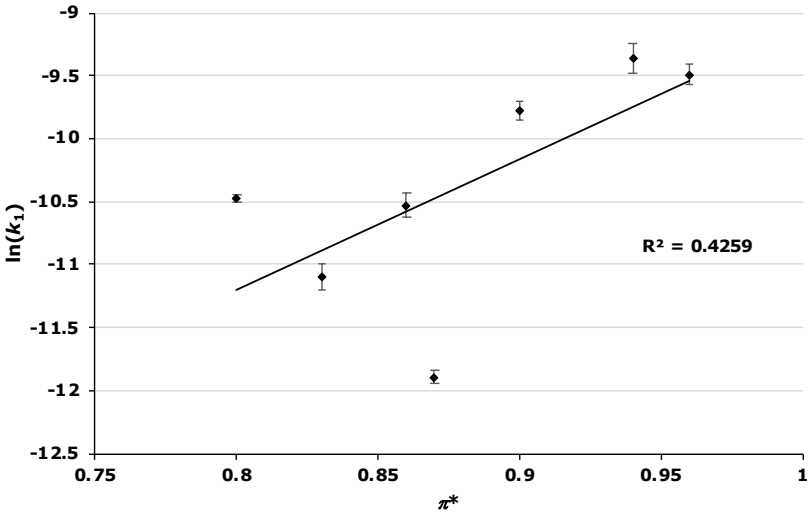

Figure S35. The relationship between the natural logarithm of the rate constant and the π^* Kamlet–Taft parameter for the solvolysis of the galactose **1** for each of the ionic liquids **3-9** at χ *ca.* 0.95. Uncertainties are calculated from the standard deviation of triplicate measurements and transformed on calculating the natural logarithm.

Multivariate regression analyses for Kamlet–Taft correlations

These analyses, based on the work of Welton *et al.*,[12] have been performed using a combination of the Kamlet–Taft parameters as outlined below in each case. They are reported in the form $\ln(k_1)$ = intercept + aα + bβ + cπ* with p-values in parentheses and italics after each coefficient.

χ *ca.* 0.01 for ionic liquids **3-9**

Combination of α, β, and π*

$\ln(k_1) = -8.48(\textit{0.00041}) + 0.25(\textit{0.73})\alpha - 3.12(\textit{0.041})\beta + 3.38(\textit{0.061})\pi^*$

Combination of α and β

$\ln(k_1) = -7.37(\textit{0.00013}) + 1.73(\textit{0.082})\alpha - 0.72(\textit{0.34})\beta$

Combination of α and π*

$\ln(k_1) = -7.62(\textit{0.00067}) + 1.90(\textit{0.10})\alpha - 0.20(\textit{0.85})\pi^*$

Combination of β and π*

$\ln(k_1) = -8.54(\textit{3.26 x } 10^{-5}) - 3.36(\textit{0.0040})\beta + 3.70(\textit{0.00531})\pi^*$

Combination of α

$\ln(k_1) = -7.75(\textit{5.25 x } 10^{-6}) + 1.80(\textit{0.069})\alpha$

Combination of β

$\ln(k_1) = -6.43(\textit{2.46 x } 10^{-5}) - 0.96(\textit{0.34})\beta$

Combination π*

$\ln(k_1) = -7.28(\textit{0.00088}) + 0.46(\textit{0.71})\pi^*$

Combination of α, β, and π*

$\ln(k_1) = 3.40(\textit{0.58})\alpha + 5.06(\textit{0.50})\beta - 12.40(\textit{0.12})\pi^*$

Combination of α and β

$\ln(k_1) = -6.74(0.076)\alpha - 7.50(0.058)\beta$

Combination of α and π^*

$\ln(k_1) = 0.47(0.91)\alpha - 8.05(0.013)\pi^*$

Combination of β and π^*

$\ln(k_1) = 2.22(0.65)\beta - 8.99(0.015)\pi^*$

χ *ca.* 0.02 for ionic liquids **3-9**

Combination of α, β, and π^* with intercept

$\ln(k_1) = -9.67(0.00081) - 0.66(0.54)\alpha - 6.35(0.017)\beta + 7.08(0.024)\pi^*$

Combination of α and β with intercept

$\ln(k_1) = -7.33(0.0018) + 2.44(0.17)\alpha - 1.33(0.36)\beta$

Combination of α and π^* with intercept

$\ln(k_1) = -7.90(0.0068) + 2.69(0.20)\alpha - 0.21(0.91)\pi^*$

Combination of β and π^* with intercept

$\ln(k_1) = -9.54(0.00011) - 5.72(0.0026)\beta + 6.22(0.0036)\pi^*$

Combination of α and intercept

$\ln(k_1) = -8.05(9.38 \times 10^{-5}) + 2.62(0.13)\alpha$

Combination of β and intercept

$\ln(k_1) = -6.03(0.00040) - 1.59(0.34)\beta$

Combination π^* and intercept

$\ln(k_1) = -7.50(0.0072) + 0.82(0.69)\pi^*$

Combination of α, β, and π^*

$\ln(k_1) = 2.98(0.67)\alpha + 3.06(0.71)\beta - 10.97(0.20)\pi^*$

Combination of α and β

$\ln(k_1) = -5.99(0.11)\alpha - 8.05(0.051)\beta$

Combination of α and π^*

$\ln(k_1) = 1.20(0.79)\alpha - 8.34(0.016)\pi^*$

Combination of β and π^*

$\ln(k_1) = 0.57(0.92)\beta - 7.98(0.035)\pi^*$

χ *ca.* 0.05 for ionic liquids **3-9**

Combination of α, β, and π^* with intercept

$\ln(k_1) = -10.55(0.0020) - 0.08(0.96)\alpha - 7.80(0.028)\beta + 8.45(0.041)\pi^*$

Combination of α and β with intercept

$\ln(k_1) = -7.75(0.0033) + 3.63(0.12)\alpha - 1.79(0.33)\beta$

Combination of α and π^* with intercept

$\ln(k_1) = -8.38(0.012) + 4.03(0.14)\alpha - 0.48(0.85)\pi^*$

Combination of β and π^* with intercept

$\ln(k_1) = -10.53(0.00026) - 7.72(0.0028)\beta + 8.36(0.0040)\pi^*$

Combination of α and intercept

$\ln(k_1) = -8.72(0.00020) + 3.87(0.090)\alpha$

Combination of β and intercept

$\ln(k_1) = -5.81(0.0019) - 2.17(0.33)\beta$

Combination π^* and intercept

$\ln(k_1) = -7.79(0.020) + 1.07(0.70)\pi^*$

Combination of α, β, and π^*

$\ln(k_1) = 3.88(0.62)\alpha + 2.47(0.79)\beta - 11.22(0.23)\pi^*$

Combination of α and β

$\ln(k_1) = -5.30(0.17)\alpha - 8.89(0.046)\beta$

Combination of α and π^*

$\ln(k_1) = 2.45(0.62)\alpha - 9.10(0.016)\pi^*$

Combination of β and π^*

$\ln(k_1) = -0.78(0.90)\beta - 7.33(0.064)\pi^*$

χ *ca.* 0.10 for ionic liquids **3-9**

Combination of α, β, and π^* with intercept

$\ln(k_1) = -12.42(0.0047) + 1.79(0.49)\alpha - 9.64(0.051)\beta + 10.24(0.078)\pi^*$

Combination of α and β with intercept

$\ln(k_1) = -9.04(0.0048) + 6.27(0.055)\alpha - 2.37(0.32)\beta$

Combination of α and π^* with intercept

$\ln(k_1) = -9.74(0.018) + 6.87(0.073)\alpha - 0.81(0.80)\pi^*$

Combination of β and π^* with intercept

$\ln(k_1) = -12.77(0.0010) - 11.36(0.0051)\beta + 12.55(0.0067)\pi^*$

Combination of α and intercept

$\ln(k_1) = -10.32(0.00031) + 6.59(0.040)\alpha$

Combination of β and intercept

$\ln(k_1) = -5.69(0.012) - 3.03(0.37)\beta$

Combination π^* and intercept

$\ln(k_1) = -8.74(0.053) + 1.82(0.66)\pi^*$

Combination of α, β, and π^*

$\ln(k_1) = 6.45(0.49)\alpha + 2.46(0.82)\beta - 12.95(0.24)\pi^*$

Combination of α and β

$\ln(k_1) = -4.14(0.34)\alpha - 10.65(0.044)\beta$

Combination of α and π^*

$\ln(k_1) = 5.03(0.40)\alpha - 10.83(0.016)\pi^*$

Combination of β and π^*

$\ln(k_1) = -2.94(0.69)\beta - 6.48(0.15)\pi^*$

χ *ca.* 0.20 for ionic liquids **3-9**

Combination of α, β, and π^* with intercept

$\ln(k_1) = -16.13(0.0054) + 2.05(0.67)\alpha - 13.76(0.045)\beta + 16.01(0.056)\pi^*$

Combination of α and β with intercept

$\ln(k_1) = -10.84(0.011) + 9.07(0.062)\alpha - 2.39(0.49)\beta$

Combination of α and π^* with intercept

$\ln(k_1) = -12.30(0.026) + 9.31(0.081)\alpha + 0.23(0.96)\pi^*$

Combination of β and π^* with intercept

$\ln(k_1) = -16.53(0.0011) - 15.75(0.0043)\beta + 18.68(0.0044)\pi^*$

Combination of α and intercept

$\ln(k_1) = -12.13(0.00070) + 9.39(0.038)\alpha$

Combination of β and intercept

$\ln(k_1) = -5.99(0.040) - 3.35(0.49)\beta$

Combination π^* and intercept

$\ln(k_1) = -10.94(0.071) + 3.81(0.51)\pi^*$

Combination of α, β, and π^*

$\ln(k_1) = 8.11(0.50)\alpha + 1.94(0.89)\beta - 14.09(0.31)\pi^*$

Combination of α and β

$\ln(k_1) = -3.41(0.51)\alpha - 12.32(0.054)\beta$

Combination of α and π^*

$\ln(k_1) = 6.99(0.37)\alpha - 12.41(0.025)\pi^*$

Combination of β and π^*

$\ln(k_1) = -4.84(0.62)\beta - 5.95(0.28)\pi^*$

χ *ca.* 0.35 for ionic liquids **3-9**

Combination of α, β, and π^* with intercept

$\ln(k_1) = -20.24(0.011) + 1.63(0.76)\alpha - 15.31(0.11)\beta + 20.96(0.091)\pi^*$

Combination of α and β with intercept

$\ln(k_1) = -13.32(0.016) + 10.81(0.092)\alpha - 0.43(0.93)\beta$

Combination of α and π^* with intercept

$\ln(k_1) = -15.98(0.022) + 9.70(0.12)\alpha + 3.40(0.55)\pi^*$

Combination of β and π^* with intercept

$\ln(k_1) = -20.56(0.0025) - 16.88(0.015)\beta + 23.07(0.0095)\pi^*$

Combination of α and intercept

$\ln(k_1) = -13.55(0.0014) + 10.87(0.055)\alpha$

Combination of β and intercept

$\ln(k_1) = -7.54(0.041) - 1.57(0.80)\beta$

Combination π^* and intercept

$\ln(k_1) = -14.56(0.043) + 7.12(0.30)\pi^*$

Combination of α, β, and π^*

$\ln(k_1) = 9.24(0.55)\alpha + 4.40(0.81)\beta - 16.82(0.34)\pi^*$

Combination of α and β

$\ln(k_1) = -4.52(0.49)\alpha - 12.64(0.096)\beta$

Combination of α and π^*

$\ln(k_1) = 6.69(0.50)\alpha - 13.04(0.049)\pi^*$

Combination of β and π^*

$\ln(k_1) = -3.33(0.78)\beta - 7.56(0.28)\pi^*$

χ *ca.* 0.50 for ionic liquids **3-9**

Combination of α, β, and π^* with intercept

$\ln(k_1) = -21.83(0.0071) + 2.14(0.67)\alpha - 12.38(0.14)\beta + 20.08(0.084)\pi^*$

Combination of α and β with intercept

$\ln(k_1) = -15.20(0.0086) + 10.93(0.078)\alpha + 1.88(0.67)\beta$

Combination of α and π^* with intercept

$\ln(k_1) = -18.39(0.0079) + 8.66(0.11)\alpha + 5.89(0.26)\pi^*$

Combination of β and π^* with intercept

$\ln(k_1) = -22.25(0.0015) - 14.44(0.021)\beta + 22.85(0.0079)\pi^*$

Combination of α and intercept

$\ln(k_1) = -14.18(0.00099) + 10.68(0.053)\alpha$

Combination of β and intercept

$\ln(k_1) = -9.36(0.018) + 0.73(0.90)\beta$

Combination π^* and intercept

$\ln(k_1) = -17.12(0.015) + 9.21(0.15)\pi^*$

Combination of α, β, and π^*

$\ln(k_1) = 10.34(0.53)\alpha + 8.87(0.65)\beta - 20.66(0.28)\pi^*$

Combination of α and β

$\ln(k_1) = -6.56(0.37)\alpha - 12.05(0.14)\beta$

Combination of α and π^*

$\ln(k_1) = 5.20(0.62)\alpha - 13.02(0.063)\pi^*$

Combination of β and π^*

$\ln(k_1) = 0.23(0.99)\beta - 10.30(0.18)\pi^*$

χ *ca.* 0.72 for ionic liquids **3-9**

Combination of α, β, and π^* with intercept

$\ln(k_1) = -23.23(0.0081) + 2.77(0.62)\alpha - 5.51(0.48)\beta + 16.59(0.15)\pi^*$

Combination of α and β with intercept

$\ln(k_1) = -17.75(0.0037) + 10.04(0.080)\alpha + 6.28(0.18)\beta$

Combination of α and π^* with intercept

$\ln(k_1) = -21.70(0.0019) + 5.68(0.17)\alpha + 10.28(0.046)\pi^*$

Combination of β and π^* with intercept

$\ln(k_1) = -23.77(0.0018) - 8.19(0.14)\beta + 20.19(0.018)\pi^*$

Combination of α and intercept

$\ln(k_1) = -14.36(0.0019) + 9.20(0.12)\alpha$

Combination of β and intercept

$\ln(k_1) = -12.38(0.0043) + 5.22(0.36)\beta$

Combination π^* and intercept

$\ln(k_1) = -20.86(0.0018) + 12.46(0.024)\pi^*$

Combination of α, β, and π^*

$\ln(k_1) = 11.50(0.51)\alpha + 17.11(0.42)\beta - 26.76(0.21)\pi^*$

Combination of α and β

$\ln(k_1) = -10.39(0.23)\alpha - 9.99(0.25)\beta$

Combination of α and π^*

$\ln(k_1) = 1.59(0.89)\alpha - 12.04(0.11)\pi^*$

Combination of β and π^*

$\ln(k_1) = 7.49(0.59)\beta - 15.22(0.086)\pi^*$

χ *ca.* 0.95 for ionic liquids **3-9**

Combination of α, β, and π^* with intercept

$\ln(k_1) = -24.75(0.0087) - 2.07(0.74)\alpha - 15.61(0.13)\beta + 25.91(0.074)\pi^*$

Combination of α and β with intercept

$\ln(k_1) = -16.20(0.016) + 9.28(0.19)\alpha + 2.79(0.62)\beta$

Combination of α and π^* with intercept

$\ln(k_1) = -20.41(0.012) + 6.16(0.31)\alpha + 8.01(0.23)\pi^*$

Combination of β and π* with intercept

$\ln(k_1) = -24.34(0.0021) - 13.61(0.044)\beta + 23.23(0.014)\pi^*$

Combination of α and intercept

$\ln(k_1) = -14.69(0.0026) + 8.91(0.16)\alpha$

Combination of β and intercept

$\ln(k_1) = -11.24(0.011) + 1.81(0.77)\beta$

Combination π* and intercept

$\ln(k_1) = -19.51(0.0093) + 10.37(0.11)\pi^*$

Combination of α, β, and π*

$\ln(k_1) = 7.24(0.69)\alpha + 8.49(0.70)\beta - 20.29(0.34)\pi^*$

Combination of α and β

$\ln(k_1) = -9.36(0.26)\alpha - 12.06(0.17)\beta$

Combination of α and π*

$\ln(k_1) = 2.32(0.85)\alpha - 12.98(0.091)\pi^*$

Combination of β and π*

$\ln(k_1) = 2.44(0.86)\beta - 13.04(0.14)\pi^*$

Multivariate regression analysis plots for each mole fraction of ionic liquids 3-9

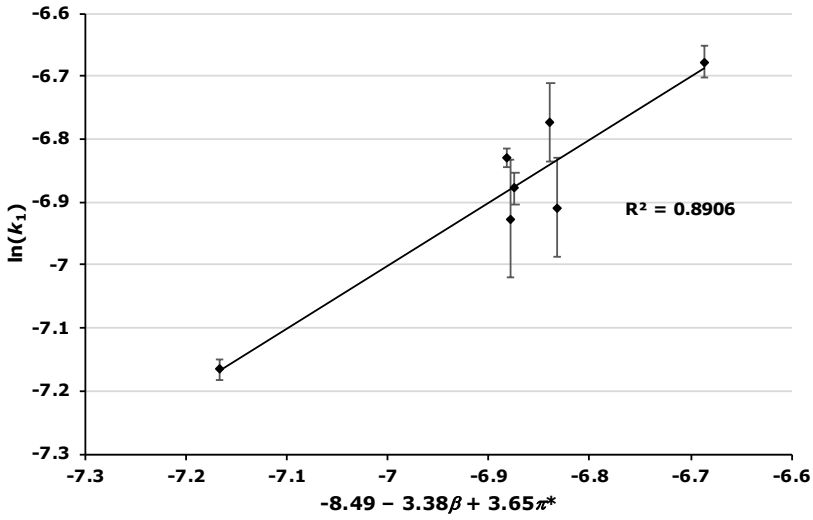

Figure S36. The relationship between the natural logarithm of the rate constant and a combination of the β and π^* Kamlet–Taft parameters for the solvolysis of the galactose **1** for each of the ionic liquids **3-9** at χ *ca.* 0.01. Uncertainties are calculated from the standard deviation of triplicate measurements and transformed on calculating the natural logarithm.

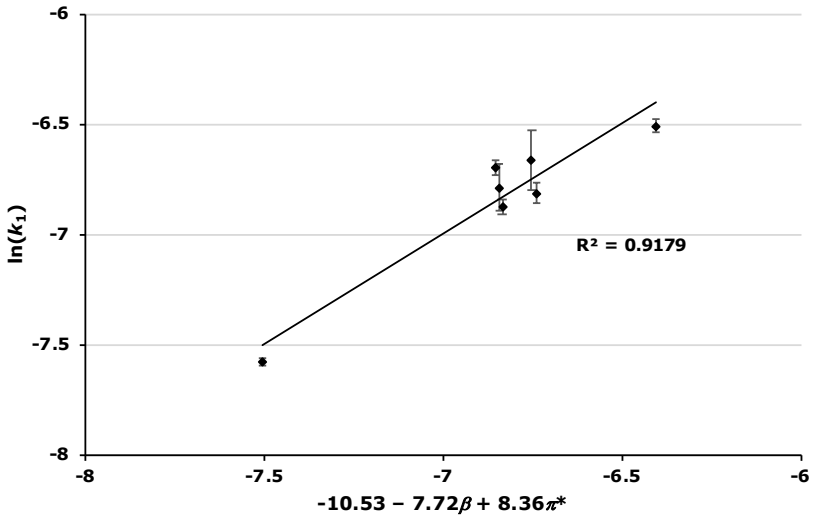

Figure S37. The relationship between the natural logarithm of the rate constant and a combination of the β and π^* Kamlet–Taft parameters for the solvolysis of the galactose **1** for each of the ionic liquids **3-9** at χ *ca.* 0.05. Uncertainties are calculated from the standard deviation of triplicate measurements and transformed on calculating the natural logarithm.

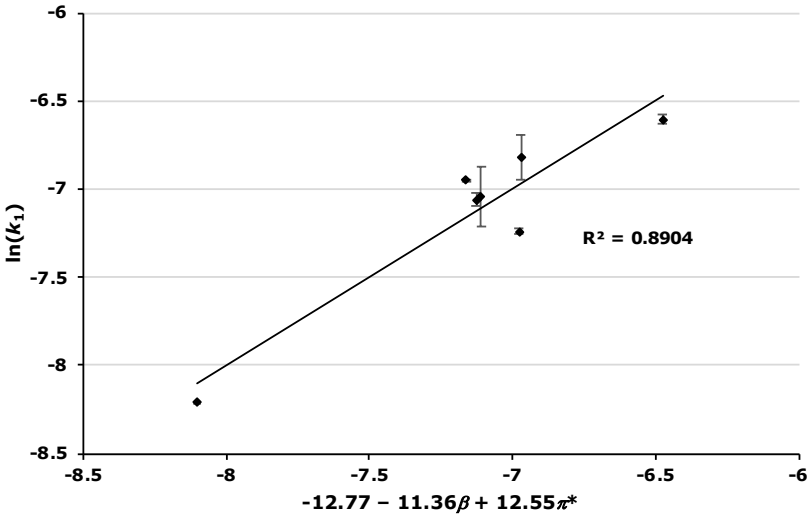

Figure S38. The relationship between the natural logarithm of the rate constant and a combination of the β and π^* Kamlet–Taft parameters for the solvolysis of the galactose **1** for each of the ionic liquids **3-9** at χ *ca.* 0.10. Uncertainties are calculated from the standard deviation of triplicate measurements and transformed on calculating the natural logarithm.

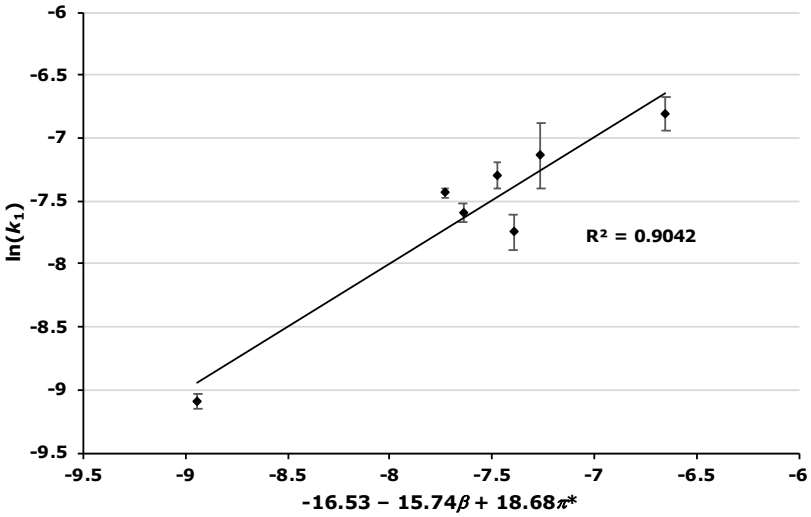

Figure S39. The relationship between the natural logarithm of the rate constant and a combination of the β and π^* Kamlet–Taft parameters for the solvolysis of the galactose **1** for each of the ionic liquids **3-9** at χ *ca.* 0.20. Uncertainties are calculated from the standard deviation of triplicate measurements and transformed on calculating the natural logarithm.

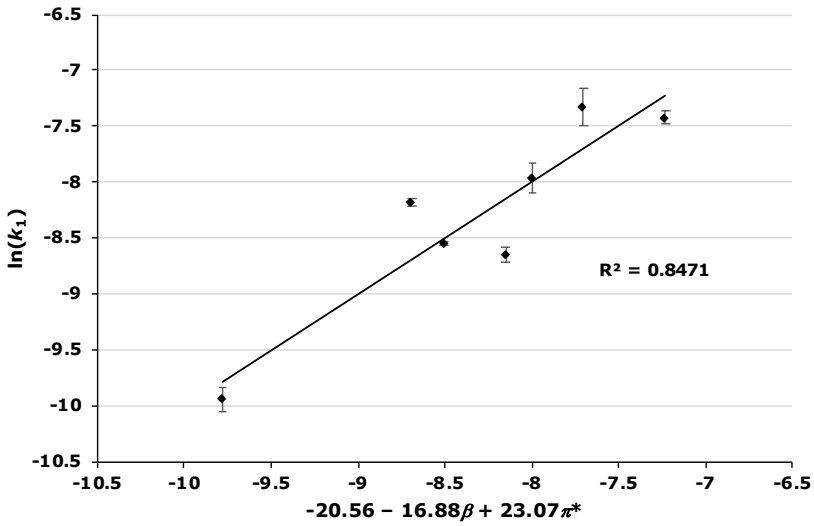

Figure S40. The relationship between the natural logarithm of the rate constant and a combination of the β and π^* Kamlet–Taft parameters for the solvolysis of the galactose **1** for each of the ionic liquids **3-9** at χ *ca.* 0.35. Uncertainties are calculated from the standard deviation of triplicate measurements and transformed on calculating the natural logarithm.

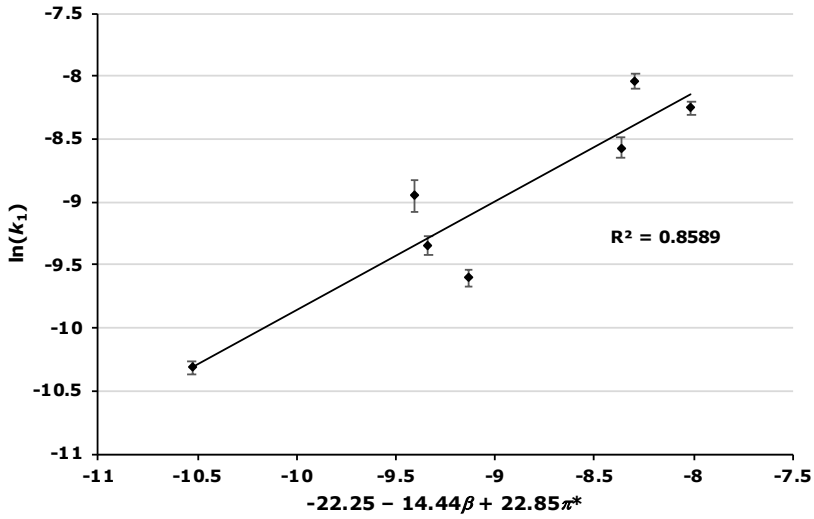

Figure S41. The relationship between the natural logarithm of the rate constant and a combination of the β and π^* Kamlet–Taft parameters for the solvolysis of the galactose **1** for each of the ionic liquids **3-9** at χ *ca.* 0.50. Uncertainties are calculated from the standard deviation of triplicate measurements and transformed on calculating the natural logarithm.

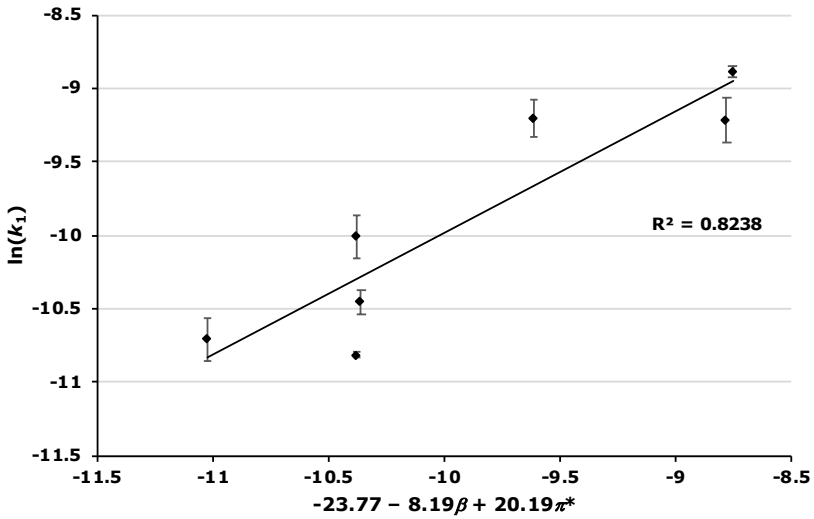

Figure S42. The relationship between the natural logarithm of the rate constant and a combination of the β and π* Kamlet–Taft parameters for the solvolysis of the galactose **1** for each of the ionic liquids **3-9** at χ *ca.* 0.73. Uncertainties are calculated from the standard deviation of triplicate measurements and transformed on calculating the natural logarithm.

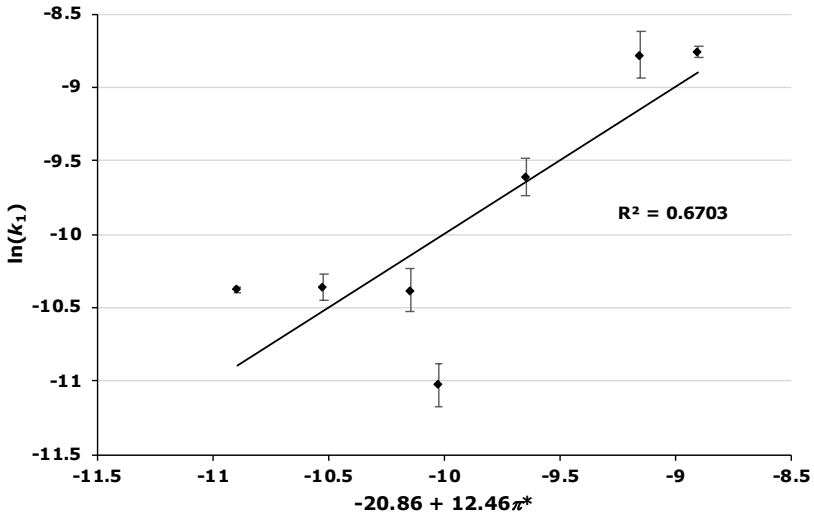

Figure S43. The relationship between the natural logarithm of the rate constant and the π* Kamlet–Taft parameter for the solvolysis of the galactose **1** for each of the ionic liquids **3-9** at χ *ca.* 0.73. Uncertainties are calculated from the standard deviation of triplicate measurements and transformed on calculating the natural logarithm.

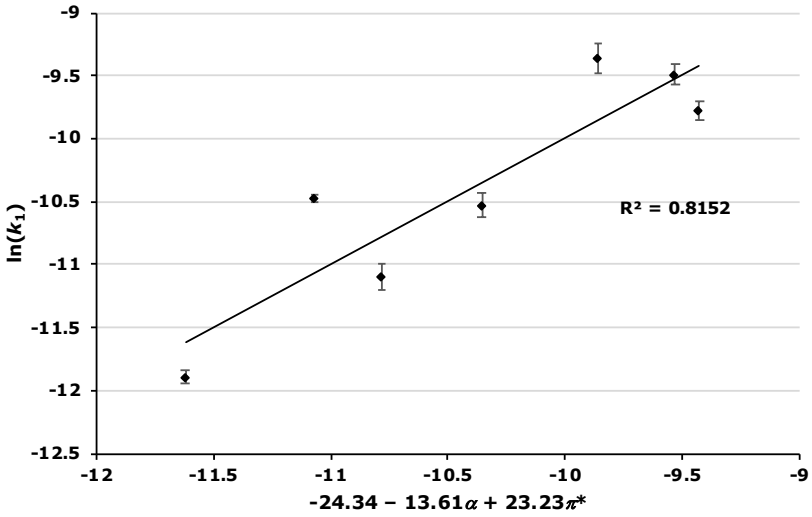

Figure S44. The relationship between the natural logarithm of the rate constant and a combination of the β and π^* Kamlet–Taft parameters for the solvolysis of the galactose **1** for each of the ionic liquids **3-9** at χ ca. 0.95. Uncertainties are calculated from the standard deviation of triplicate measurements and transformed on calculating the natural logarithm.

Investigation of alternative methods for Kamlet–Taft correlations

As mentioned in the main text, it is clear that the methanol solvent is a having a greater effect on these relationships than has been seen previously. Several alternative methods of finding significant relationships between the rate constants and the Kamlet–Taft parameters were investigated for this reason. Initially, the Kamlet–Taft parameters of methanol were considered to be included in the fits; this would result in an equation for each mole fraction where:

$$\ln(k_1) = \text{intercept} + a\alpha_{MeOH} + b\beta_{MeOH} + c\pi^*_{MeOH} + d\alpha_{IL} + e\beta_{IL} + f\pi^*_{IL}$$

This is clearly unreasonable given that the rate constants of the seven studied ionic liquids would be fitted to seven variables and therefore any significant results would be justifiably questionable.

Instead, parameters unique to each solvent composition were investigated. That is, the parameters of both methanol and each ionic liquid would be weighted for each mole fraction to give an effective parameter. For example, for the case of $\chi = 0.20$, $\alpha_{eff} = 0.2a_{IL} + 0.8a_{MeOH}$; $\beta_{eff} = 0.2\beta_{IL} + 0.8\beta_{MeOH}$; $\pi^*_{eff} = 0.2\pi^*_{IL} + 0.8\pi^*_{MeOH}$. Given the range of the values of the rate constants at low mole fractions, it was deemed unnecessary to consider these weighted values at $\chi = 0.01$-0.10 as the effective parameters would consist almost completely of the methanol parameters. Therefore, the effective parameters were considered only at $\chi = 0.20$ and above. The results are shown below in Table S1.

Table S1. The correlation between $\ln(k_1)$ and the Kamlet–Taft parameters β_{eff} and π^*_{eff} across each mole fraction of the ionic liquids **3-9**.

Mole fraction	$\ln(k_1)$	R^2 (adjusted)
0.20	no significant fit	N/A
0.35	$-26.02 - 48.24\beta + 65.91\pi^*$	0.77
0.50	$-26.67 - 28.88\beta + 45.70\pi^*$	0.79
0.73	$-26.47 - 11.37\beta + 28.04\pi^*$	0.74
0.95	$-24.62 - 14.33\beta + 24.45\pi^*$	0.73

It is clear from these results that weighting these parameters to better reflect the solvent composition does not improve these relationships as observed in the adjusted R^2 values. In addition, given no significant fit was found for $\chi = 0.20$ this approach is clearly not useful at lower mole fractions. In addition, as seen in the main text, the coefficient of the β parameter in the $\chi = 0.73$ case has a p-value of 0.14 indicating it is not a significant fit. Again, a significant relationship is found with the π^* parameter and intercept alone.

A final method was investigated to see if a better fit for these correlations could be observed. A few key studies have measured the parameters of a mixtures of ionic liquids and several molecular solvents. One of these studies[13] measured the parameters of mixtures of dimethylformamide and the ionic liquid *N*-methyl-*N*-(2-methoxyethyl)pyrrolidinium lysinate. This study only reported the β and π^* values and found that the β parameter is the same as that of the pure ionic liquid above $\chi = 0.10$, while the π^* parameter changed as though in an ideal mixture across mole fractions of the ionic liquid. Because of these results, analyses were carried out using the weighted π^* parameter and the β parameter of the pure ionic liquids. These found significant relationships as outlined in Table S2.

Table S2. The correlation between $\ln(k_1)$ and the Kamlet–Taft parameters β and π^*_{eff} across each mole fraction of the ionic liquids **3-9**.

Mole fraction	$\ln(k_1)$	R^2 (adjusted)
0.20	no significant fit	N/A
0.35	$-46.77 - 16.89\beta + 65.91\pi^*$	0.77
0.50	$-36.23 - 14.44\beta + 45.70\pi^*$	0.79
0.73	$-28.58 - 8.18\beta + 28.04\pi^*$	0.74
0.95	$-25.09 - 13.61\beta + 24.45\pi^*$	0.72

These results are similar to those displayed in Table 1 where all parameters were weighted for each mole fraction; again, this does not improve the significance of these relationships above those fits found when using the parameters of the pure ionic liquids. In addition, again the relationship shown at $\chi = 0.73$ is not significant for the β parameter (p-value = 0.13) but a significant relationship was found for the π^* parameter in this particular case. The full analyses for these two methods are shown below the following paragraphs.

A previous study[14] measured the Kamlet–Taft parameters of mixtures of 1,3-dimethyl-2-imidazolidinone (DMI) and the ionic liquid 1-ethyl-3-methylimidazolium acetate ([emim][OAc]). This study found that at $\chi = 0.20$ and above, both the β and π^* parameters were the same as those of the pure ionic liquid, while the α parameter increased with increasing amounts of ionic liquid in the reaction mixture, acting like an ideal mixture of the two solvents; that is the above weighting method was not an unreasonable attempt to model the solvent properties for these mixtures. Because of these results, the above method of weighting the parameters was attempted for $\chi = 0.20$ and above only for α, keeping both β and π^* parameters as the values of the neat ionic liquids. No significant fits were found using this method and because of this, the data are not included here.

Finally, a recent study[15] using protic ionic liquids in mixtures with methanol found that across mole fractions, both the α and β parameters acted like an ideal mixture. Unlike the above study, this was not found for the π^* parameter. In this case, up until χ *ca.* 0.20 (where the solvent is 80% methanol by moles) the π^* parameter deviated from ideality towards that of neat ionic liquid. Because of this, the above method of weighting the parameters was again attempted without any changes to the π^* parameters at $\chi > 0.20$ (i.e. using that of each ionic liquid with no incorporation of the methanol π^* parameter). Again, no significant fits were found using this method and the data are not included here for this reason.

Below are the multivariate regression analyses for the effective Kamlet–Taft parameters, each parameter weighted as detailed above for each solvent composition. They are displayed in the form $\ln(k_1) = \text{intercept} + a\alpha_{eff} + b\beta_{eff} + c\pi^*_{eff}$ with p-values in parentheses and italics after each coefficient.

χ *ca.* 0.20 for ionic liquids **3-9**

Combination of α_{eff}, β_{eff}, and π^*_{eff} with intercept

$\ln(k_1) = -32.74(\textit{0.24}) + 14.11(\textit{0.49})\alpha - 50.51(\textit{0.29})\beta + 66.31(\textit{0.27})\pi^*$

Combination of α_{eff} and β_{eff} with intercept

$\ln(k_1) = -43.92(\textit{0.13}) + 43.14(\textit{0.11})\alpha - 3.44(\textit{0.86})\beta$

Combination of α_{eff} and π^*_{eff} with intercept

$\ln(k_1) = -49.50(0.068) + 40.73(0.14)\alpha + 8.38(0.74)\pi^*$

Combination of β_{eff} and π^*_{eff} with intercept

$\ln(k_1) = -23.82(0.12) - 64.13(0.060)\beta + 84.58(0.045)\pi^*$

Combination of α_{eff} and intercept

$\ln(k_1) = -46.48(0.037) + 43.60(0.065)\alpha$

Combination of β_{eff} and intercept

$\ln(k_1) = -2.59(0.87) - 7.99(0.75)\beta$

Combination π^*_{eff} and intercept

$\ln(k_1) = -23.57(0.24) + 24.01(0.40)\pi^*$

Combination of α_{eff}, β_{eff}, and π^*_{eff}

$\ln(k_1) = -19.75(0.36)\alpha - 83.02(0.083)\beta + 93.00(0.15)\pi^*$

Combination of α_{eff} and β_{eff}

$\ln(k_1) = 8.67(0.53)\alpha - 24.52(0.24)\beta$

Combination of α_{eff} and π^*_{eff}

$\ln(k_1) = 3.05(0.90)\alpha - 15.47(0.63)\pi^*$

Combination of β_{eff} and π^*_{eff}

$\ln(k_1) = -63.74(0.095)\beta + 48.44(0.16)\pi^*$

χ *ca.* 0.35 for ionic liquids **3-9**

Combination of α_{eff}, β_{eff}, and π^*_{eff} with intercept

$\ln(k_1) = -28.24(0.062) + 4.66(0.76)\alpha - 43.75(0.11)\beta + 59.88(0.091)\pi^*$

Combination of α_{eff} and β_{eff} with intercept

$\ln(k_1) = -32.74(0.084) + 30.88(0.092)\alpha - 1.23(0.93)\beta$

Combination of α_{eff} and π^*_{eff} with intercept

$\ln(k_1) = 5.06(0.80) - 7.46(0.74)\alpha - 10.30(0.67)\pi^*$

Combination of β_{eff} and π^*_{eff} with intercept

$\ln(k_1) = -26.02(0.013) - 48.24(0.015)\beta + 65.91(0.0095)\pi^*$

Combination of α_{eff} and intercept

$\ln(k_1) = -33.61(0.021) + 31.04(0.055)\alpha$

Combination of β_{eff} and intercept

$\ln(k_1) = -5.61(0.59) - 4.49(0.80)\beta$

Combination π^*_{eff} and intercept

$\ln(k_1) = -22.66(0.13) + 20.35(0.30)\pi^*$

Combination of α_{eff}, β_{eff}, and π^*_{eff}

$\ln(k_1) = -24.01(0.24)\alpha - 67.66(0.082)\beta + 73.22(0.14)\pi^*$

Combination of α_{eff} and β_{eff}

$\ln(k_1) = 3.45(0.74)\alpha - 18.58(0.22)\beta$

Combination of α_{eff} and π^*_{eff}

$\ln(k_1) = -3.93(0.80)\alpha - 7.21(0.69)\pi^*$

Combination of β_{eff} and π^*_{eff}

$\ln(k_1) = -41.50(0.15)\beta + 23.37(0.31)\pi^*$

χ *ca.* 0.50 for ionic liquids **3-9**

Combination of α_{eff}, β_{eff}, and π^*_{eff} with intercept

$\ln(k_1) = -28.05(0.016) + 4.27(0.67)\alpha - 24.76(0.14)\beta + 40.17(0.084)\pi^*$

Combination of α_{eff} and β_{eff} with intercept

$\ln(k_1) = -27.31(0.036) + 21.86(0.078)\alpha + 3.67(0.67)\beta$

Combination of α_{eff} and π^*_{eff} with intercept

$\ln(k_1) = -30.60(0.014) + 17.32(0.11)\alpha + 11.77(0.26)\pi^*$

Combination of β_{eff} and π^*_{eff} with intercept

$\ln(k_1) = -26.67(0.0036) - 28.88(0.021)\beta + 45.70(0.0079)\pi^*$

Combination of α_{eff} and intercept

$\ln(k_1) = -24.80(0.011) + 21.36(0.053)\alpha$

Combination of β_{eff} and intercept

$\ln(k_1) = -9.84(0.19) + 1.45(0.90)\beta$

Combination π^*_{eff} and intercept

$\ln(k_1) = -22.75(0.036) + 18.42(0.15)\pi^*$

Combination of α_{eff}, β_{eff}, and π^*_{eff}

$\ln(k_1) = -19.10(0.40)\alpha - 38.46(0.29)\beta + 36.21(0.43)\pi^*$

Combination of α_{eff} and β_{eff}

$\ln(k_1) = -2.65(0.76)\alpha - 12.36(0.30)\beta$

Combination of α_{eff} and π^*_{eff}

$\ln(k_1) = -1.23(0.94)\alpha - 10.82(0.50)\pi^*$

Combination of β_{eff} and π^*_{eff}

$\ln(k_1) = -17.36(0.46)\beta + 1.21(0.95)\pi^*$

χ *ca.* 0.72 for ionic liquids **3-9**

Combination of α_{eff}, β_{eff}, and π^*_{eff} with intercept

$\ln(k_1) = -26.83(0.0082) + 3.85(0.62)\alpha - 7.65(0.48)\beta + 23.05(0.15)\pi^*$

Combination of α_{eff} and β_{eff} with intercept

$\ln(k_1) = -23.25(0.0092) + 13.95(0.080)\alpha + 8.72(0.18)\beta$

Combination of α_{eff} and π^*_{eff} with intercept

$\ln(k_1) = -26.34(0.0029) + 7.88(0.17)\alpha + 14.28(0.046)\pi^*$

Combination of β_{eff} and π^*_{eff} with intercept

$\ln(k_1) = -26.47(0.0023) - 11.37(0.14)\beta + 28.04(0.018)\pi^*$

Combination of α_{eff} and intercept

$\ln(k_1) = -17.91(0.0089) + 12.78(0.12)\alpha$

Combination of β_{eff} and intercept

$\ln(k_1) = -13.72(0.016) + 7.25(0.36)\beta$

Combination π^*_{eff} and intercept

$\ln(k_1) = -23.83(0.0028) + 17.31(0.024)\pi^*$

Combination of α_{eff}, β_{eff}, and π^*_{eff}

$\ln(k_1) = -2.99(0.90)\alpha + 1.01(0.98)\beta - 10.57(0.78)\pi^*$

Combination of α_{eff} and β_{eff}

$\ln(k_1) = -9.26(0.28)\alpha - 7.65(0.44)\beta$

Combination of α_{eff} and π^*_{eff}

$\ln(k_1) = -3.55(0.80)\alpha - 9.47(0.41)\pi^*$

Combination of β_{eff} and π^*_{eff}

$\ln(k_1) = 4.06(0.83)\beta - 14.89(0.27)\pi^*$

χ *ca.* 0.95 for ionic liquids **3-9**

Combination of α_{eff}, β_{eff}, and π^*_{eff} with intercept

$\ln(k_1) = -24.93(0.0088) - 2.17(0.74)\alpha - 16.43(0.13)\beta + 27.27(0.074)\pi^*$

Combination of α_{eff} and β_{eff} with intercept

$\ln(k_1) = -16.78(0.019) + 9.77(0.19)\alpha + 2.93(0.62)\beta$

Combination of α_{eff} and π^*_{eff} with intercept

$\ln(k_1) = -20.99(0.012) + 6.49(0.31)\alpha + 8.43(0.23)\pi^*$

Combination of β_{eff} and π^*_{eff} with intercept

$\ln(k_1) = -24.62(0.0022) - 14.33(0.044)\beta + 24.45(0.014)\pi^*$

Combination of α_{eff} and intercept

$\ln(k_1) = -15.16(0.0035) + 9.38(0.16)\alpha$

Combination of β_{eff} and intercept

$\ln(k_1) = -11.30(0.014) + 1.90(0.77)\beta$

Combination π^*_{eff} and intercept

$\ln(k_1) = -19.84(0.010) + 10.92(0.11)\pi^*$

Combination of α_{eff}, β_{eff}, and π^*_{eff}

$\ln(k_1) = 5.34(0.78)\alpha + 6.38(0.79)\beta - 18.61(0.44)\pi^*$

Combination of α_{eff} and β_{eff}

$\ln(k_1) = -9.06(0.27)\alpha - 11.68(0.19)\beta$

Combination of α_{eff} and π^*_{eff}

$\ln(k_1) = 1.62(0.89)\alpha - 12.85(0.12)\pi^*$

Combination of β_{eff} and π^*_{eff}

$\ln(k_1) = 1.73(0.91)\beta - 12.87(0.17)\pi^*$

Below are the multivariate regression analyses for the Kamlet–Taft parameters with the π^* parameter weighted as detailed above for each solvent composition. They are displayed in the form $\ln(k_1)$ = intercept + $b\beta$ + $c\pi^*_{eff}$ with p-values in parentheses and italics after each coefficient.

χ *ca.* 0.20 for ionic liquids **3-9**

Combination of β and π^*_{eff} with intercept

$\ln(k_1) = -57.78(0.031) - 12.83(0.060)\beta + 84.58(0.045)\pi^*$

Combination π^*_{eff} and intercept

$\ln(k_1) = -23.57(0.24) + 24.01(0.40)\pi^*$

Combination of β and π^*_{eff}

$\ln(k_1) = -0.97(0.87)\beta - 10.69(0.047)\pi^*$

χ *ca.* 0.35 for ionic liquids **3-9**

Combination of β and π^*_{eff} with intercept

$\ln(k_1) = -46.78(0.0053) - 16.89(0.015)\beta + 65.91(0.0096)\pi^*$

Combination π^*_{eff} and intercept

$\ln(k_1) = -22.66(0.13) + 20.35(0.30)\pi^*$

Combination of β and π^*_{eff}

$\ln(k_1) = -0.98(0.91)\beta - 11.07(0.091)\pi^*$

χ *ca.* 0.50 for ionic liquids **3-9**

Combination of β and π^*_{eff} with intercept

$\ln(k_1) = -36.23(0.0029) - 14.44(0.021)\beta + 45.70(0.0079)\pi^*$

Combination π^*_{eff} and intercept

$\ln(k_1) = -22.75(0.036) + 18.42(0.15)\pi^*$

Combination of β and π^*_{eff}

$\ln(k_1) = 2.02(0.83)\beta - 13.33\ (0.069)\pi^*$

χ *ca.* 0.72 for ionic liquids **3-9**

Combination of β and π^*_{eff} with intercept

$\ln(k_1) = -28.58(0.0029) - 8.19(0.14)\beta + 28.04(0.018)\pi^*$

Combination π^*_{eff} and intercept

$\ln(k_1) = -23.83(0.0028) + 17.31(0.024)\pi^*$

Combination of β and π^*_{eff}

$\ln(k_1) = 8.37(0.48)\beta + 17.19(0.045)\pi^*$

χ *ca.* 0.95 for ionic liquids **3-9**

Combination of β and π^*_{eff} with intercept

$\ln(k_1) = -25.09(0.0023) - 13.61(0.044)\beta + 24.45(0.014)\pi^*$

Combination π^*_{eff} and intercept

$\ln(k_1) = -19.84(0.010) + 10.92(0.11)\pi^*$

Combination of β and π^*_{eff}

$\ln(k_1) = 2.74(0.84)\beta - 13.40(0.12)\pi^*$

Multivariate regression analysis plots with weighted parameters for each mole fraction of ionic liquids 3-9

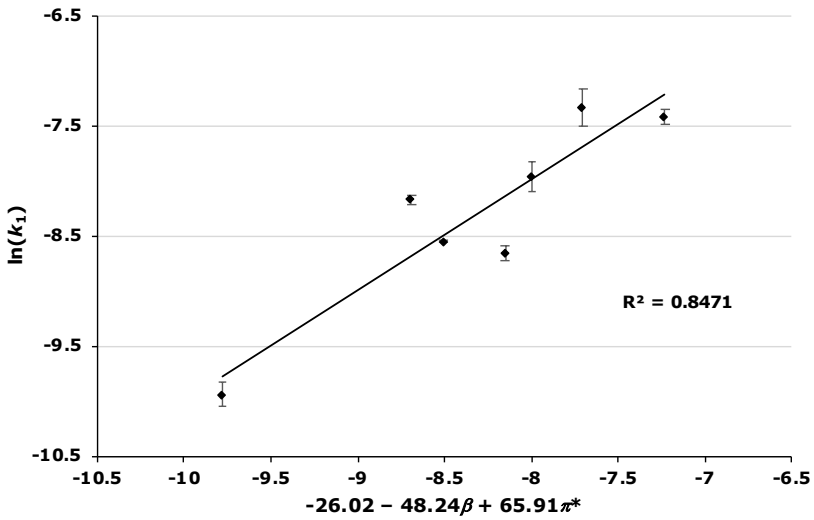

Figure S45. The relationship between the natural logarithm of the rate constant and a combination of the β_{eff} and π^*_{eff} Kamlet–Taft parameters for the solvolysis of the galactose **1** for each of the ionic liquids **3-9** at χ *ca.* 0.35. Uncertainties are calculated from the standard deviation of triplicate measurements and transformed on calculating the natural logarithm.

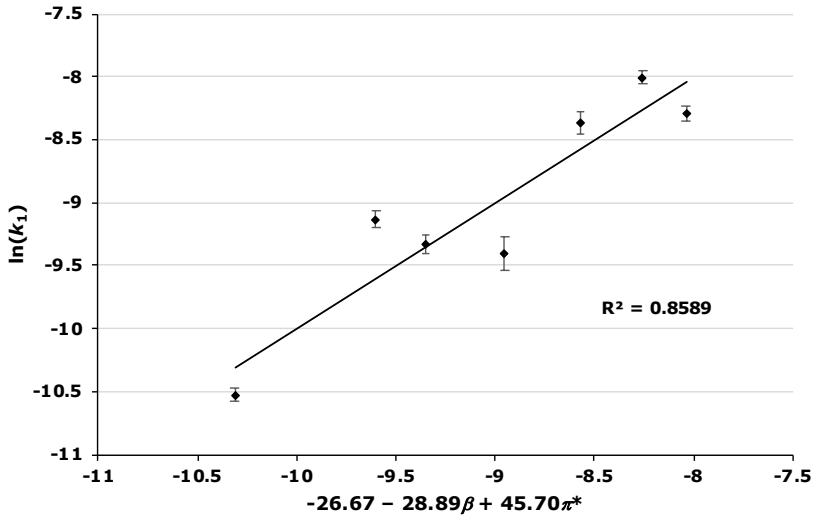

Figure S46. The relationship between the natural logarithm of the rate constant and a combination of the β_{eff} and π^*_{eff} Kamlet–Taft parameters for the solvolysis of the galactose **1** for each of the ionic liquids **3-9** at χ *ca.* 0.50. Uncertainties are calculated from the standard deviation of triplicate measurements and transformed on calculating the natural logarithm.

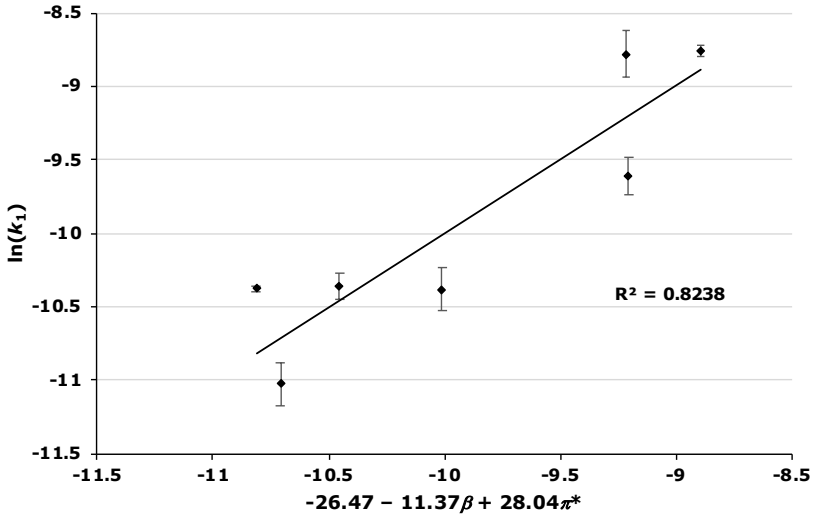

Figure S47. The relationship between the natural logarithm of the rate constant and a combination of the β_{eff} and π^*_{eff} Kamlet–Taft parameters for the solvolysis of the galactose **1** for each of the ionic liquids **3-9** at χ *ca.* 0.73. Uncertainties are calculated from the standard deviation of triplicate measurements and transformed on calculating the natural logarithm.

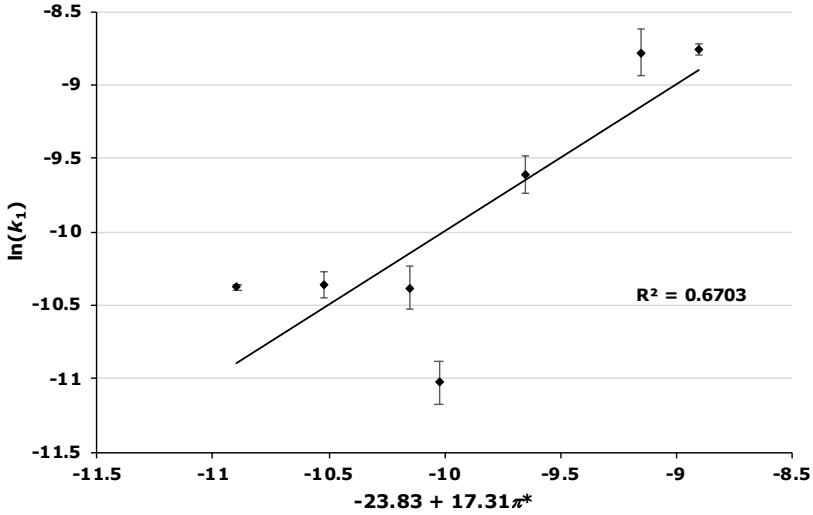

Figure S48. The relationship between the natural logarithm of the rate constant and the π^*_{eff} Kamlet–Taft parameter for the solvolysis of the galactose **1** for each of the ionic liquids **3-9** at χ *ca.* 0.73. Uncertainties are calculated from the standard deviation of triplicate measurements and transformed on calculating the natural logarithm.

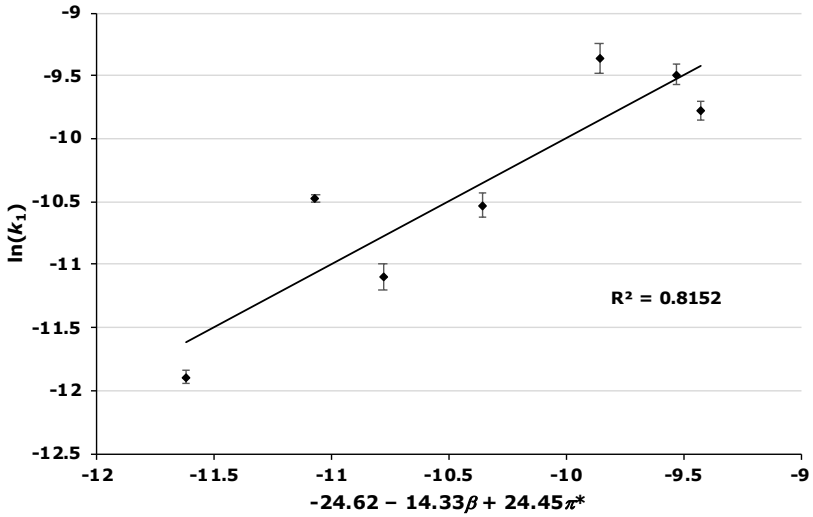

Figure S49. The relationship between the natural logarithm of the rate constant and a combination of the β_{eff} and π^*_{eff} Kamlet–Taft parameters for the solvolysis of the galactose **1** for each of the ionic liquids **3-9** at χ *ca.* 0.95. Uncertainties are calculated from the standard deviation of triplicate measurements and transformed on calculating the natural logarithm.

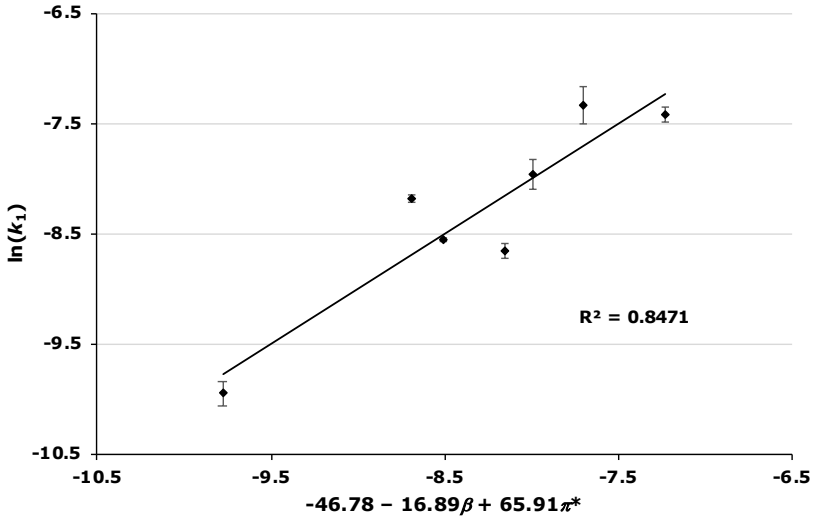

Figure S50. The relationship between the natural logarithm of the rate constant and a combination of the β and π^*_{eff} Kamlet–Taft parameters for the solvolysis of the galactose **1** for each of the ionic liquids **3-9** at χ *ca.* 0.35. Uncertainties are calculated from the standard deviation of triplicate measurements and transformed on calculating the natural logarithm.

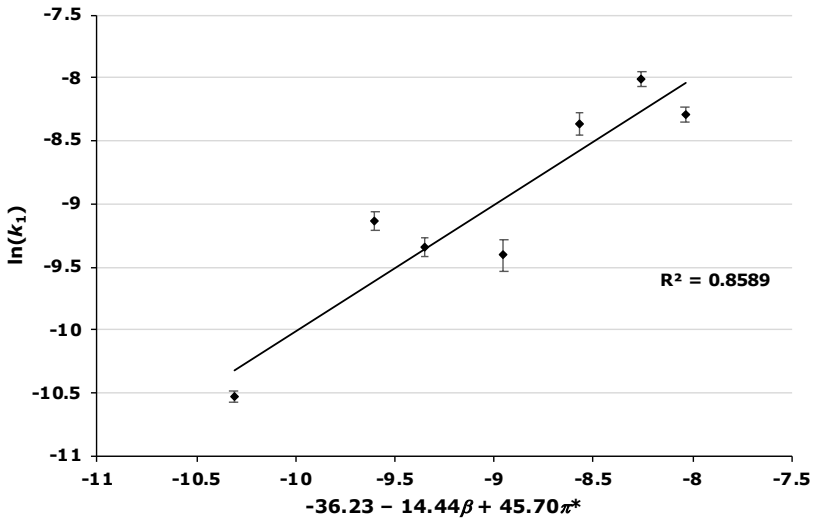

Figure S51. The relationship between the natural logarithm of the rate constant and a combination of the β and π^*_{eff} Kamlet–Taft parameters for the solvolysis of the galactose **1** for each of the ionic liquids **3-9** at χ *ca.* 0.50. Uncertainties are calculated from the standard deviation of triplicate measurements and transformed on calculating the natural logarithm.

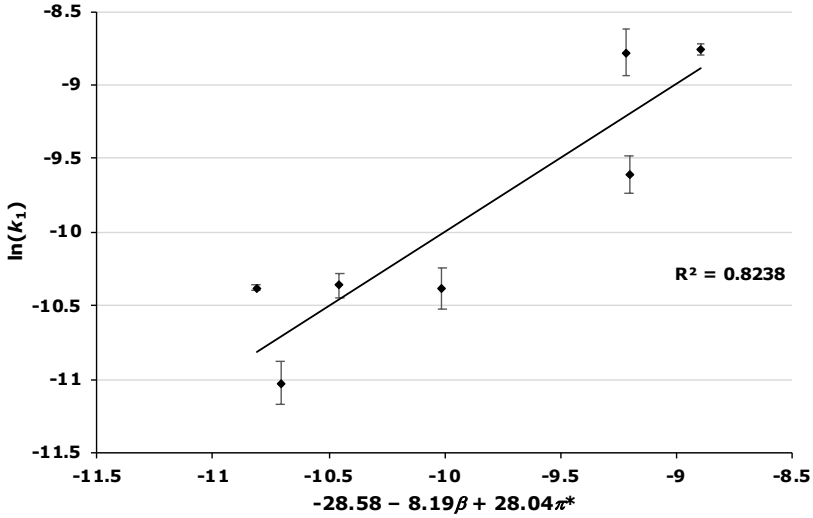

Figure S52. The relationship between the natural logarithm of the rate constant and a combination of the β and π^*_{eff} Kamlet–Taft parameters for the solvolysis of the galactose **1** for each of the ionic liquids **3-9** at χ *ca.* 0.73. Uncertainties are calculated from the standard deviation of triplicate measurements and transformed on calculating the natural logarithm.

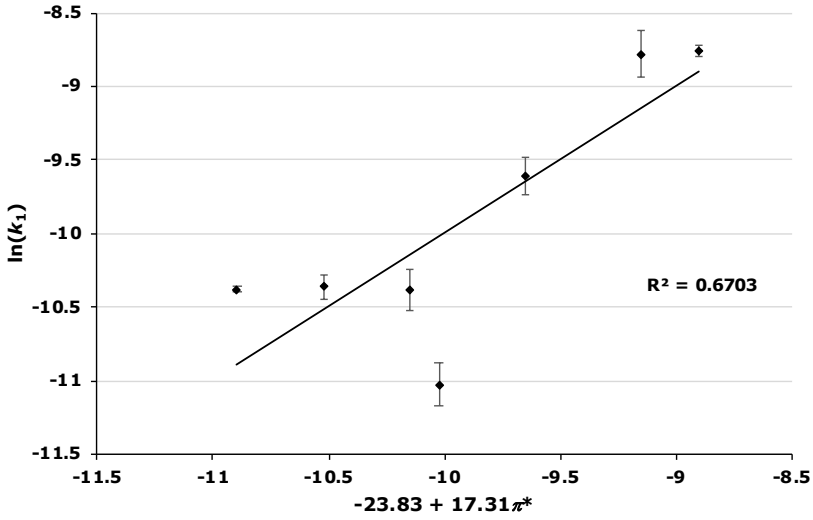

Figure S53. The relationship between the natural logarithm of the rate constant and the π^*_{eff} Kamlet–Taft parameter for the solvolysis of the galactose **1** for each of the ionic liquids **3-9** at χ *ca.* 0.73. Uncertainties are calculated from the standard deviation of triplicate measurements and transformed on calculating the natural logarithm.

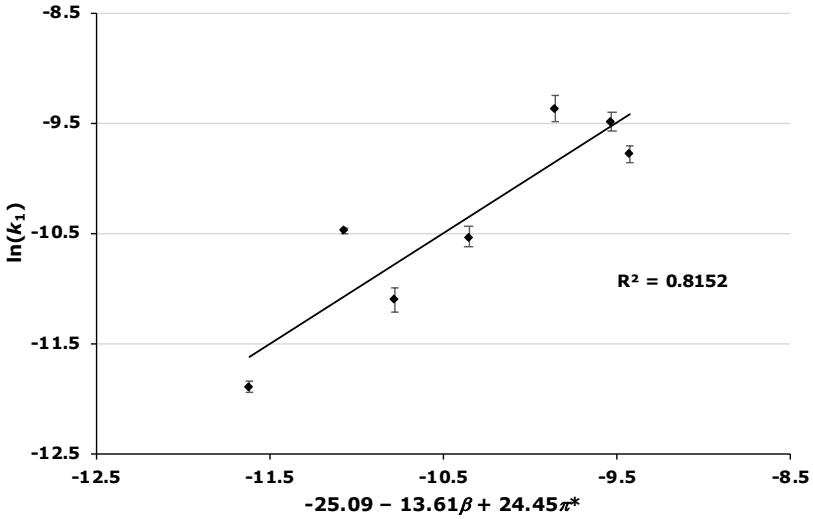

Figure S54. The relationship between the natural logarithm of the rate constant and a combination of the β and π^*_{eff} Kamlet–Taft parameters for the solvolysis of the galactose **1** for each of the ionic liquids **3-9** at χ *ca.* 0.95. Uncertainties are calculated from the standard deviation of triplicate measurements and transformed on calculating the natural logarithm.

Product ratios for the reaction of galactose 1 in mixtures containing each ionic liquid 3-9

The product ratios for [bmim][BF4] **8** and [bmim][C(CN)$_3$] **9** are not included in this analysis as there was evidence of adventitious water reacting to give the product 2,3,4,6-tetra-*O*-acetyl-*β*-D-galactopyranose **13** (Figure S50) in addition to products **2** and **10-12** as seen in other ionic liquids **3-7**. As with all ionic liquids, salts **8** and **9** were dried under reduced pressure (<0.20 mbar) for at least 6 hours before use in all cases and the water content was found to be <300 ppm using Karl Fischer coulometry. The formation of this product in addition to the ratios of additional products **10-12** was inconsistent between different batches of both of these ionic liquids; importantly, the differences in the rate constants for these batches was negligible. Although product **13** was not isolated, it was confirmed using ^{1}H NMR spectroscopy by the doublet at *ca.* 5.5 ppm with $J = 9.7$ Hz, which matches reported literature.[16] Mass spectrometry also confirmed the presence of this product (HRMS (ESI) calculated for $C_{14}H_{20}O_{10}$ $[M+Na]^+$: 371.10; found 371.0948).

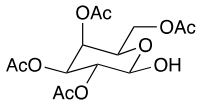

13

Figure S50. 2,3,4,6-Tetra-*O*-acetyl-*β*-D-galactopyranose **13**.

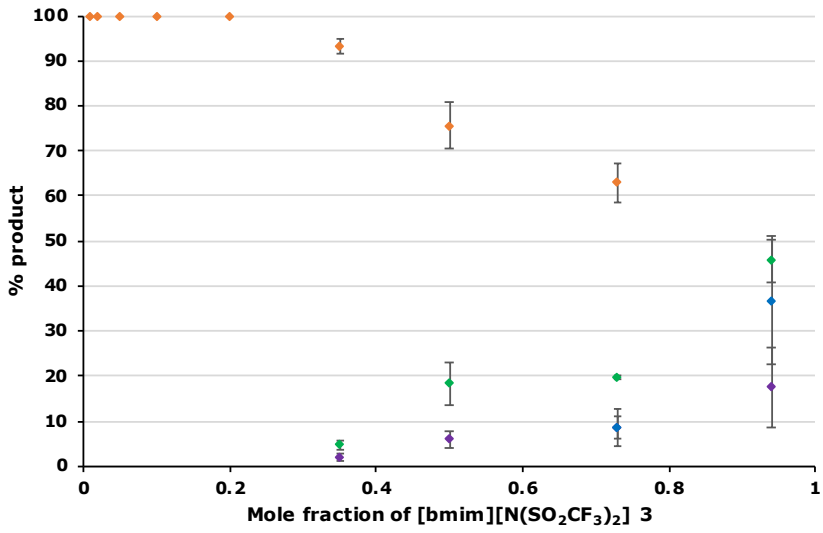

Figure S55. The ratio of each product **2** (♦), **10** (♦), **11** (♦) or **12** (♦) for the reaction of the galactose **1** in mixtures of methanol and [bmim][N(SO$_2$CF$_3$)$_2$] **3**. Uncertainties were determined from the standard deviation of triplicate measurements.

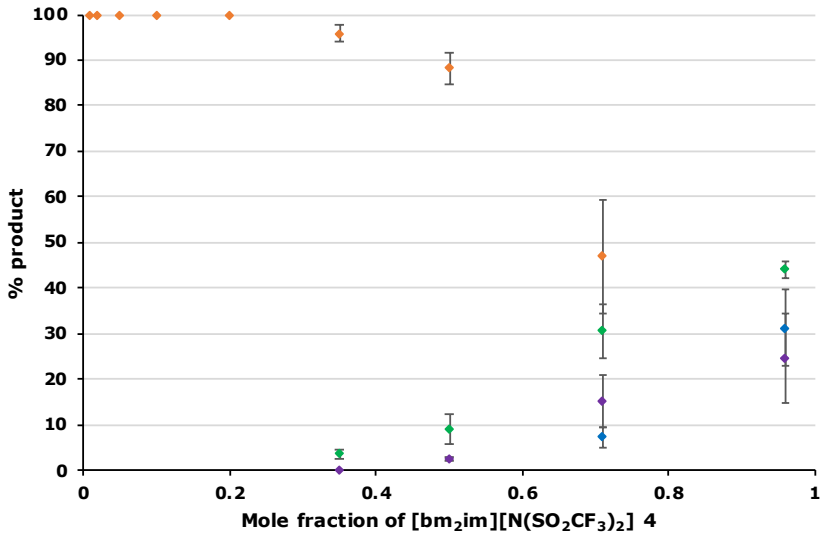

Figure S56. The ratio of each product **2** (♦), **10** (♦), **11** (♦) or **12** (♦) for the reaction of the galactose **1** in mixtures of methanol and $[bm_2im][N(SO_2CF_3)_2]$ **4**. Uncertainties were determined from the standard deviation of triplicate measurements.

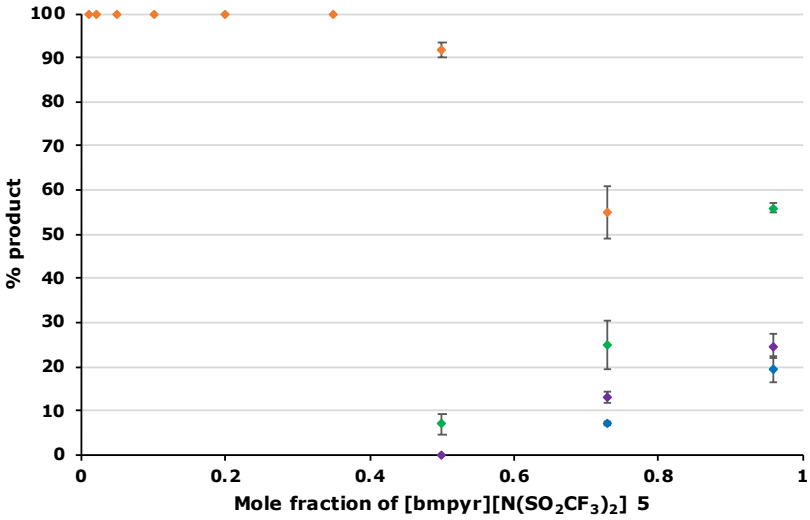

Figure S57. The ratio of each product **2** (♦), **10** (♦), **11** (♦) or **12** (♦) for the reaction of the galactose **1** in mixtures of methanol and $[bmpyr][N(SO_2CF_3)_2]$ **5**. Uncertainties were determined from the standard deviation of triplicate measurements.

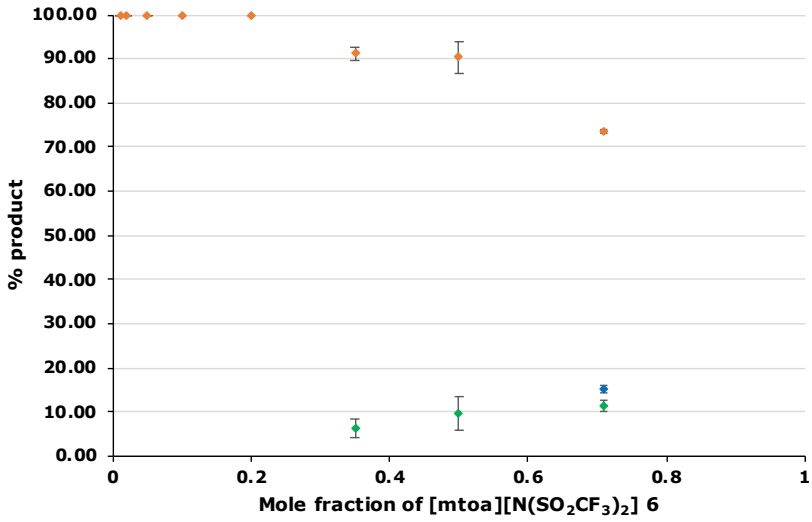

Figure S58. The ratio of each product **2** (♦), **10** (♦), **11** (♦) or **12** (♦) for the reaction of the galactose **1** in mixtures of methanol and [mtoa][$N(SO_2CF_3)_2$] **6**. Uncertainties were determined from the standard deviation of triplicate measurements. Large uncertainties and absence of product **11** percentages in some solvent compositions are due to poor signal to noise ratios for mixtures containing ionic liquid **6**.

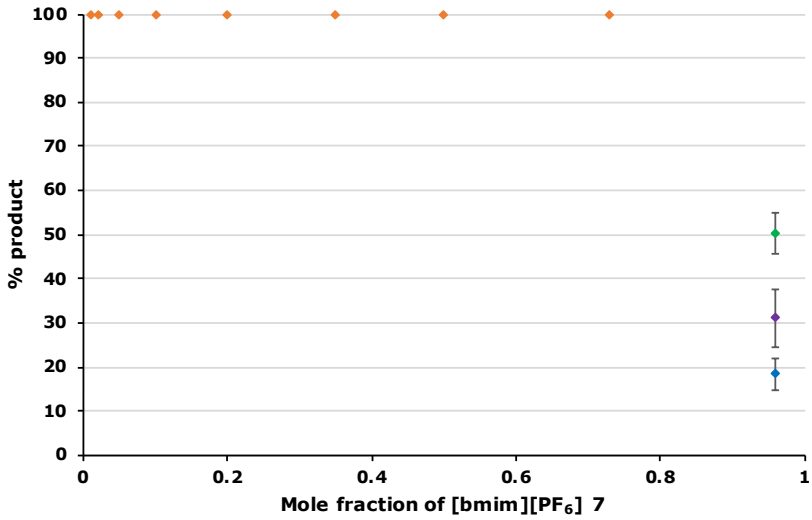

Figure S59. The ratio of each product **2** (♦), **10** (♦), **11** (♦) or **12** (♦) for the reaction of the galactose **1** in mixtures of methanol and [bmim][PF_6] **7**. Uncertainties were determined from the standard deviation of triplicate measurements.

Table S3. The mole fraction of [bmim][$N(SO_2CF_3)_2$] **3** and the per cent of each product **2**, **10, 11** and **12**. Uncertainties were determined from the standard deviation of triplicate measurements.

χ_3	% **2**	% **10**	% **11**	% **12**
0	100	0	0	0
0.01	100	0	0	0
0.02	100	0	0	0
0.07	100	0	0	0
0.12	100	0	0	0
0.20	100	0	0	0
0.37	93 ± 2	5 ± 1	2 ± 1	0
0.50	76 ± 5	18 ± 5	6 ± 2	0
0.72	63 ± 4	20 ± 1	9 ± 3	9 ± 4
0.93	0	46 ± 5	18 ± 9	37 ± 14

Table S4. The mole fraction of [bm_2im][$N(SO_2CF_3)_2$] **4** and the per cent of each product **2**, **10**, **11** and **12**. Uncertainties were determined from the standard deviation of triplicate measurements.

χ_4	% **2**	% **10**	% **11**	% **12**
0.01	100	0	0	0
0.02	100	0	0	0
0.03	100	0	0	0
0.06	100	0	0	0
0.10	100	0	0	0
0.21	100	0	0	0
0.36	96 ± 2	3 ± 1	trace	0
0.48	88 ± 4	9 ± 3	3 ± 1	0
0.71	47 ± 12	31 ± 6	15 ± 6	7 ± 2
0.95	0	44 ± 2	25 ± 10	31 ± 9

Table S5. The mole fraction of [bmpyr][$N(SO_2CF_3)_2$] **5** and the per cent of each product **2**, **10**, **11** and **12**. Uncertainties were determined from the standard deviation of triplicate measurements.

χ_5	% **2**	% **10**	% **11**	% **12**
0.01	100	0	0	0
0.03	100	0	0	0
0.05	100	0	0	0
0.11	100	0	0	0
0.18	100	0	0	0
0.32	100	0	0	0
0.48	92 ± 2	7 ± 2	trace	0
0.71	55 ± 6	25 ± 6	13 ± 1	7 ± 1
0.93	0	56 ± 1	25 ± 3	20 ± 3

Table S6. The mole fraction of [mtoa][$N(SO_2CF_3)_2$] **6** and the per cent of each product **2**, **10**, **11** and **12**. Uncertainties were determined from the standard deviation of triplicate measurements. Large uncertainties and absence of product **11** percentages in some solvent compositions are due to poor signal to noise ratios for mixtures containing ionic liquid **6**.

χ_6	% **2**	% **10**	% **11**	% **12**
0.01	100	0	0	0
0.03	100	0	0	0
0.05	100	0	0	0
0.11	100	0	0	0
0.18	100	0	0	0
0.32	91 ± 1	6 ± 2	trace	0
0.48	90 ± 4	10 ± 4	trace	0
0.71	74 ± 1	11 ± 1	trace	15 ± 1

Table S7. The mole fraction of [bmim][PF_6] **7** and the per cent of each product **2**, **10**, **11** and **12**. Uncertainties were determined from the standard deviation of triplicate measurements.

χ_7	% **2**	% **10**	% **11**	% **12**
0.02	100	0	0	0
0.03	100	0	0	0
0.06	100	0	0	0
0.12	100	0	0	0
0.21	100	0	0	0
0.33	100	0	0	0
0.51	100	0	0	0
0.74	100	0	0	0
0.96	0	50 ± 5	31 ± 7	18 ± 4

Experimental details for isolation studies

All isolation studies were performed in triplicate for each solvent composition with descriptions below. Due to the small scale of the reactions, products were generally isolated as oils rather than solids as detailed in literature. Product identities were confirmed using ^{1}H NMR spectroscopy and mass spectrometry (details below).

Methanol case ($\chi_{IL} = 0$)

Acetobromogalactose **1** (*ca.* 10 mg, 0.024 mmol) and triethylamine (*ca.* 10 mg, 0.10 mmol) were dissolved in methanol (3 mL). The solution was heated to 42 °C for 2 hours. ^{1}H NMR spectroscopy was used to confirm that the extent of conversion was greater than 95%. The methanol was removed *in vacuo* and the crude mixture was dissolved in dichloromethane (0.5 mL). The solution was eluted through a plug of silica (3:2, hexane/ethyl acetate) to give methyl 2,3,4,6-tetra-*O*-acetyl-*β*-D-galactopyranoside **2** as a colourless oil (*ca.* 8.0 mg, 87-93%). ^{1}H NMR (CD_3CN, 400 MHz). δ 1.92–2.10 (4 x s, 12H, $COCH_3$), 3.44 (s, 3H, OCH_3), 3.99-4.07 (m, 2H, H5 & H6b), 4.13-4.17 (m, 1H, H6a), 4.48 (d, J = 7.5 Hz, 1H, H1), 4.97-5.06 (m, 2H, H2 & H3), 5.33 (dd, J = 1.2, 3.3 Hz, H4) which matched that previously reported.[17]

[Bmim][BF_4] **8** χ_{IL} *ca.* 0.02 case

Acetobromogalactose **1** (*ca.* 10 mg, 0.024 mmol) and triethylamine (*ca.* 10 mg, 0.10 mmol) were dissolved in methanol (3 mL). [Bmim][BF_4] **8** (*ca.* 0.50 g, 2.0 mmol) was added. The solution was heated to 42 °C for 1 hour. ^{1}H NMR spectroscopy was used to confirm that the extent of conversion was greater than 95%. The methanol was removed *in vacuo* and the crude mixture was dissolved in dichloromethane (0.5 mL). The solution was eluted through a plug of silica (3:2, hexane/ethyl acetate) to give the product, methyl 2,3,4,6-tetra-*O*-acetyl-*β*-D-galactopyranoside **2** as a colourless oil (*ca.* 8.0 mg, 90-97%) with ^{1}H NMR spectral data as reported above.

[Bmim][$N(SO_2CF_3)_2$] **3** χ_{IL} *ca.* 0.02 case

Acetobromogalactose **1** (*ca.* 10 mg, 0.024 mmol) and triethylamine (*ca.* 10 mg, 0.10 mmol) were dissolved in methanol (3 mL). [Bmim][$N(SO_2CF_3)_2$] **3** (*ca.* 1.0 g, 2.4 mmol) was added.

The solution was heated to 42 °C for 1 hour. ^{1}H NMR spectroscopy was used to confirm that the extent of conversion was greater than 95%. The methanol was removed *in vacuo* and the crude mixture was dissolved in dichloromethane (0.5 mL). The solution was eluted through a plug of silica (3:2, hexane/ethyl acetate) to give the product, methyl 2,3,4,6-tetra-*O*-acetyl-*β*-D-galactopyranoside **2** as a colourless oil (*ca.* 8.0 mg, 78-98%) with ^{1}H NMR spectral data as reported above.

[Bmim][$N(SO_2CF_3)_2$] **3** χ_{IL} *ca.* 0.32 case

Acetobromogalactose **1** (*ca.* 100 mg, 0.24 mmol) and triethylamine (*ca.* 60 mg, 0.60 mmol) were dissolved in methanol (0.18 mL). [Bmim][$N(SO_2CF_3)_2$] **3** (*ca.* 1.0 g, 2.4 mmol) was added and the solution was heated to 42 °C for 5 hours. ^{1}H NMR spectroscopy was used to confirm that the extent of conversion was greater than 95%. The methanol was removed *in vacuo* and dichloromethane (0.5 mL) was added was added to the residue. The mixture was purified by flash column chromatography (silica, 3:2 diethyl ether/cyclohexane) to give methyl 2,3,4,6-tetra-*O*-acetyl-*β*-D-galactopyranoside **2** as a colourless oil (*ca.* 20 mg, 19-26%) and a mixture of 3,4,6-tri-*O*-acetyl-*α*-D-galactopyranose 1,2-(*exo*-methyl orthoacetate) **10** and 3,4,6-tri-*O*-acetyl-*α*-D-galactopyranose 1,2-(*endo*-methyl orthoacetate) **11** (*ca.* 30 mg, 27-43% combined). Spectral data for compound **10**: ^{1}H NMR (CD_3CN, 500 MHz). δ 1.59 (s, 3H, CH_3), 2.00-2.06 (3 x s, 9H, $COCH_3$), 3.22 (s, 3H, -OCH_3), 4.02-4.19 (m, 2H, H6), 4.29-4.31 (m, 1H, H5), 4.35-4.37 (m, 1H, H2), 5.01-5.03 (m, 1H, H3), 5.35-5.36 (m, 1H, H4), 5.81 (d, J = 4.8 Hz, 1H, H1), which matched that previously reported.[18] Spectral data for compound **11**: ^{1}H NMR (CD_3CN, 500 MHz). δ 1.51 (s, 3H, CH_3), 1.99-2.07 (3 x s, 9H, $COCH_3$), 3.30 (s, 3H, -OCH_3), 4.02-4.19 (m, 2H, H6), 4.22-4.26 (m, 1H, H2), 4.28-4.31 (m, 1H, H5), 5.28 (m, 1H, H3), 5.37-5.38 (m, 1H, H4), 5.67 (d, J = 4.8 Hz, 1H, H1), which matched that previously reported.[18] HRMS (ESI) calculated for $C_{15}H_{22}O_{10}$ $[M+Na]^+$: 385.11; found 385.1104. The ^{1}H NMR spectral data for compound **2** matched that reported above.

[Bmim][$N(SO_2CF_3)_2$] **3** χ_{IL} *ca.* 0.76 case

Acetobromogalactose **1** (*ca.* 100 mg, 0.24 mmol) and triethylamine (*ca.* 40 mg, 0.40 mmol) were dissolved in methanol (0.08 mL). [Bmim][$N(SO_2CF_3)_2$] **3** (*ca.* 4.0 g, 9.5 mmol) was added and the solution was heated to 42 °C for 45 hours. ^{1}H NMR spectroscopy was used to confirm

that the extent of conversion was greater than 95%. The methanol was removed *in vacuo* and dichloromethane (0.5 mL) was added to the residue. The mixture was purified by flash column chromatography (silica, 3:2 diethyl ether/cyclohexane) to give methyl 2,3,4,6-tetra-*O*-acetyl-β-D-galactopyranoside **2** as a colourless oil (*ca.* 4.0 mg, 2-6%) and a mixture of 3,4,6-tri-*O*-acetyl-α-D-galactopyranose 1,2-(*exo*-methyl orthoacetate) **10**, 3,4,6-tri-*O*-acetyl-α-D-galactopyranose 1,2-(*endo*-methyl orthoacetate) **11** and 2,3,4,6-tetra-*O*-acetyl-1,5-anhydro-D-lyxo-hex-1-enitol **12** (*ca.* 50 mg, 30-51% combined). Spectral data for compound **12**: ^{1}H NMR (CD_3CN, 500 MHz). δ 1.97-2.07 (4 x s, 12H, $COCH_3$), 4.15-4.19 (m, 1H, H6a), 4.25-4.26 (m, 1H, H6b), 4.38-4.40 (m, 1H, H5), 5.40 (dd, J = 1.6, 5.0 Hz, 1H, H4), 5.83 (m, 1H, H3), 6.66 (d, J = 1.6 Hz, 1H, H1), which matched that previously reported.[19] HRMS (ESI) calculated for $C_{14}H_{18}O_9$ $[M+Na]^+$: 353.28; found 353.27. The ^{1}H NMR spectral data for compounds **2**, **10** and **11** matched those reported above.

Rate data for the nucleophile dependence study

Table S8. The exact amounts of acetonitrile, methanol, the galactose **1** and triethylamine, the concentration of methanol and the observed rate constant (k_{obs}) for the process.

Mass acetonitrile / g	Mass methanol / g	Mass galactose **1** / g	Mass NEt_3 / g	[MeOH] / mol L^{-1}	k_{obs} / 10^{-6} s^{-1}
1.541	0.0077	0.0039	0.0034	0.120	3.57
					4.19
					3.36
1.526	0.0148	0.0041	0.0050	0.231	4.01
					3.36
					2.64
1.523	0.0206	0.0039	0.0045	0.321	3.73
					4.31
					3.61
1.519	0.0293	0.0035	0.0051	0.457	3.72
					4.35
					3.48

Rate data for mole fraction dependence studies

Table S9. The mole fraction of [bmim][$N(SO_2CF_3)_2$] **3**, the exact amounts of ionic liquid **3**, methanol, the galactose **1** and triethylamine, and the first order rate constant (k_1) for the process.

χ_3	Mass ionic liquid / g	Mass methanol / g	Mass galactose **1** / g	Mass triethylamine / g	k_1 / 10^{-4} s^{-1}
0	0	1.759	0.0042	0.0025	7.79
					7.61
					7.92
0.01	0.223	1.629	0.0044	0.0038	10.1
					10.2
					10.6
0.02	0.439	1.500	0.0045	0.0038	10.9
					11.3
					11.0
0.07	1.085	1.099	0.0035	0.0043	10.2
					10.0
					10.7
0.12	1.501	0.844	0.0047	0.0045	8.62
					8.24
					8.88
0.20	1.926	0.573	0.0047	0.0048	4.89
					4.74
					5.46
0.38	2.386	0.302	0.0047	0.0048	1.90
					1.96
					1.95
0.50	2.554	0.197	0.0034	0.0036	0.89
					0.94
					0.81
0.72	2.728	0.081	0.0043	0.0050	0.30

0.93	2.854	0.013	0.0046	0.0053	0.35 0.30 0.15 0.17 0.14

Table S10. The mole fraction of $[bm_2im][N(SO_2CF_3)_2]$ **4**, the exact amounts of ionic liquid **4**, methanol, the galactose **1** and triethylamine, and the first order rate constant (k_1) for the process.

χ_4	Mass ionic liquid / g	Mass methanol / g	Mass galactose **1** / g	Mass triethylamine / g	k_1 / 10^{-4} s^{-1}
0.01	0.240	1.614	0.0037	0.0035	9.09
					10.4
					10.5
0.02	0.418	1.504	0.0039	0.0058	13.3
					12.1
					12.1
0.03	0.587	1.402	0.0037	0.0054	12.4
					13.3
					13.8
0.06	1.023	1.145	0.0046	0.0055	11.4
					11.2
					10.4
0.10					7.08
					7.26
					7.19
0.21	1.971	0.552	0.0038	0.0039	5.02
					3.96
					4.00
0.36	2.337	0.301	0.0041	0.0049	1.61
					1.83

					1.79
0.48	2.501	0.199	0.0037	0.0036	0.70
					0.86
					0.90
0.71	2.685	0.081	0.0040	0.0046	0.26
					0.34
					0.33
0.95					0.30
					0.25
					0.26

Table S11. The mole fraction of [bmpyr][$N(SO_2CF_3)_2$] **5**, the exact amounts of ionic liquid **5**, methanol, the galactose **1** and triethylamine, and the first order rate constant (k_1) for the process.

χ_5	Mass ionic liquid / g	Mass methanol / g	Mass galactose **1** / g	Mass triethylamine / g	k_1 / 10^{-4} s^{-1}
0.01	0.246	1.603	0.0052	0.0042	10.6
					10.8
					11.0
0.03	0.557	1.402	0.0044	0.0042	12.0
					11.9
					12.0
0.05	0.849	1.213	0.0049	0.0066	12.1
					12.1
					12.8
0.11	1.370	0.885	0.0036	0.0053	9.65
					9.58
					9.53
0.18	1.804	0.606	0.0039	0.0048	5.93
					6.14
					5.71
0.32	2.208	0.350	0.0038	0.0055	2.92

					2.81
					2.72
0.47	2.439	0.203	0.0038	0.0059	1.04
					1.04
					1.16
0.71	2.630	0.079	0.0036	0.0051	0.31
					0.32
					0.31
0.93	2.713	0.013	0.0056	0.0055	0.29
					0.29
					0.27

Table S12. The mole fraction of [mtoa][$N(SO_2CF_3)_2$] **6**, the exact amounts of ionic liquid **6**, methanol, the galactose **1** and triethylamine, and the first order rate constant (k_1) for the process.

χ_6	Mass ionic liquid / g	Mass methanol / g	Mass galactose **1** / g	Mass triethylamine / g	k_1 / 10^{-4} s^{-1}
0.01	0.418	1.419	0.0042	0.0059	7.61
					7.72
					7.86
0.02	0.622	1.257	0.0045	0.0057	6.59
					6.55
					6.60
0.05	0.954	1.003	0.0038	0.0048	5.09
					5.22
					5.06
0.10	1.440	0.610	0.0038	0.0044	2.74
					2.72
					2.70
0.19	1.747	0.357	0.0040	0.0039	1.09
					1.10

					1.21
0.32	1.941	0.202	0.0048	0.0053	0.43
					0.53
					0.48
0.45	2.021	0.122	0.0040	0.0051	0.28
					0.27
					0.25
0.72	2.133	0.040	0.0037	0.0058	0.14
					0.17
					0.19
0.92	2.179	0.008	0.0042	0.0071	0.072
					0.068
					0.065

Table S13. The mole fraction of [bmim][PF_6] **7**, the exact amounts of ionic liquid **7**, methanol, the galactose **1** and triethylamine, and the first order rate constant (k_1) for the process.

χ_7	Mass ionic liquid / g	Mass methanol / g	Mass galactose **1** / g	Mass triethylamine / g	k_1 / 10^{-4} s^{-1}
0.01	0.229	1.606	0.0046	0.0054	12.8
					12.2
					12.8
0.03	0.376	1.510	0.0051	0.0054	13.9
					14.3
					14.0
0.06	0.699	1.304	0.0042	0.0038	14.5
					14.8
					15.4
0.12	1.156	1.005	0.0043	0.0061	13.9
					13.3
					13.5

0.21	1.631	0.709	0.0044	0.0057	9.37
					12.0
					11.9
0.33	2.009	0.453	0.0043	0.0052	6.30
					5.58
					6.08
0.51	2.307	0.253	0.0035	0.0052	2.53
					2.63
					2.35
0.72	2.538	0.102	0.0046	0.0040	0.63
					0.61
					0.77
0.95	2.671	0.013	0.0055	0.0052	0.55
					0.61
					0.53

Table S14. The mole fraction of [bmim][BF_4] **8**, the exact amounts of ionic liquid **8**, methanol, the galactose **1** and triethylamine, and the first order rate constant (k_1) for the process.

χ_8	Mass ionic liquid / g	Mass methanol / g	Mass galactose **1** / g	Mass triethylamine / g	k_1 / 10^{-4} s^{-1}
0.01	0.139	1.642	0.0038	0.0061	12.1
					10.7
					11.6
0.02	0.205	1.609	0.0045	0.0048	11.1
					10.9
					10.9
0.04	0.388	1.467	0.0035	0.0057	13.4
					12.7
					12.8
0.06	0.547	1.347	0.0042	0.0077	12.9

					10.9
					14.4
0.10	0.874	1.142	0.0037	0.0047	10.6
					12.4
					9.79
0.23	1.444	0.702	0.0046	0.0058	8.87
					9.43
					5.61
0.33	1.725	0.151	0.0042	0.0047	7.75
					6.14
					5.70
0.48	1.972	0.299	0.0042	0.0057	3.46
					3.13
					3.37
0.67	2.186	0.151	0.0036	0.0049	1.51
					1.61
					1.61
0.95	2.355	0.015	0.0042	0.0054	0.82
					0.72
					0.72

Table S15. The mole fraction of [bmim][$C(CN)_3$] **9**, the exact amounts of ionic liquid **9**, methanol, the galactose **1** and triethylamine, and the first order rate constant (k_1) for the process.

χ_9	Mass ionic liquid / g	Mass methanol / g	Mass galactose **1** / g	Mass triethylamine / g	k_1 / 10^{-4} s^{-1}
0.01	0.185	1.601	0.0037	0.0057	8.76
					10.2
					10.5
0.03	0.342	1.470	0.0045	0.0052	13.9
					14.3

					14.0
0.06	0.552	1.298	0.0038	0.0045	12.6
					10.4
					10.8
0.12	0.882	1.010	0.0038	0.0077	10.0
					7.12
					9.23
0.21	1.248	0.670	0.0037	0.0054	7.61
					6.16
					6.56
0.36	1.613	0.400	0.0038	0.0057	3.27
					4.01
					3.14
0.49	1.767	0.251	0.0049	0.0052	2.10
					2.46
					2.42
0.72	1.936	0.101	0.0043	0.0043	1.81
					1.42
					1.38
0.94	2.031	0.015	0.0050	0.0042	0.78
					0.97
					0.81

Rate data for temperature dependence studies

Table S16. The mole fraction of [bmim][$N(SO_2CF_3)_2$] **3**, the temperature, the exact amounts of ionic liquid **3**, methanol, the galactose **1**, and triethylamine, and the first order rate constant (k_1) for the process.

χ_3	Temp / °C	Mass ionic liquid / g	Mass MeOH / g	Mass galactose **1** / g	Mass NEt_3 / g	k_1 / 10^{-4} s^{-1}
0	33.4	0	4.400	0.011	0.012	3.57
						3.80
						3.58
	42.0					7.90
						8.09
						7.70
	50.2					17.0
						16.0
						15.8
	58.2					33.6
						33.5
						31.5
0.02	33.4	1.006	3.814	0.010	0.011	5.26
						6.30
						5.54
	42.0					11.8
						12.1
						11.8
	50.2					23.1
						22.5
						22.4
	58.2					41.1
						43.0
						45.2
0.46	33.4	6.352	0.498	0.010	0.010	0.43
						0.43

						0.46
	42.0					0.97
						0.91
						0.83
	50.2					1.82
						1.88
						1.77
	58.2					4.15
						3.24
						3.66

Table S17. The mole fraction of $[bm_2im][N(SO_2CF_3)_2]$ **4**, the temperature, the exact amounts of ionic liquid **4**, methanol, the galactose **1**, and triethylamine, and the first order rate constant (k_1) for the process.

χ_4	Temp / °C	Mass ionic liquid / g	Mass MeOH / g	Mass galactose **1** / g	Mass NEt_3 / g	k_1 / 10^{-4} s^{-1}
0.02	33.4	1.074	3.750	0.011	0.010	4.95
						5.29
						5.63
	42.0					11.6
						9.53
						10.2
	50.2					18.4
						18.3
						22.1
	58.2					42.5
						45.5
						44.5
0.48	33.4	12.56	1.016	0.021	0.022	0.52
						0.46
						0.49
	42.0					0.70

						0.86
						0.90
	50.2					1.66
						1.80
						1.58
	58.2					2.79
						2.48
						3.38

Table S18. The mole fraction of [bmpyr][$N(SO_2CF_3)_2$] **5**, the temperature, the exact amounts of ionic liquid **5**, methanol, the galactose **1**, and triethylamine, and the first order rate constant (k_1) for the process.

χ_5	Temp / °C	Mass ionic liquid / g	Mass MeOH / g	Mass galactose **1** / g	Mass NEt_3 / g	k_1 / 10^{-4} s^{-1}
0.02	33.4	2.374	7.387	0.021	0.023	6.47
						5.70
						5.57
	42.0					12.5
						12.2
						12.2
	50.2					23.4
						24.0
						23.7
	58.2					45.8
						45.3
						45.2
0.48	33.4	12.29	1.001	0.020	0.022	0.46
						0.48
						0.52
	42.0					1.09
						1.07
						1.09

	50.2					2.06
						2.19
						2.18
	58.2					4.16
						4.10
						4.09

Table S19. The mole fraction of [mtoa][$N(SO_2CF_3)_2$] **6**, the temperature, the exact amounts of ionic liquid **6**, methanol, the galactose **1**, and triethylamine, and the first order rate constant (k_1) for the process.

χ_6	Temp / °C	Mass ionic liquid / g	Mass MeOH / g	Mass galactose **1** / g	Mass NEt_3 / g	k_1 / 10^{-4} s^{-1}
0.02	33.4	1.615	3.148	0.011	0.010	3.08
						3.03
						2.90
	42.0					6.59
						6.55
						6.60
	50.2					15.1
						15.0
						14.6
	58.2					28.3
						28.9
						29.0
0.45	33.4	5.131	0.308	0.010	0.011	0.18
						0.19
						0.19
	42.0	2.021	0.122	0.004	0.005	0.28
						0.27
						0.25
	50.2	5.131	0.308	0.010	0.011	0.36
						0.36
						0.37

Table S20. The mole fraction of [bmim][PF_6] **7**, the temperature, the exact amounts of ionic liquid **7**, methanol, the galactose **1**, and triethylamine, and the first order rate constant (k_1) for the process.

χ_7	Temp / °C	Mass ionic liquid / g	Mass MeOH / g	Mass galactose **1** / g	Mass NEt_3 / g	k_1 / 10^{-4} s^{-1}
0.02	33.4	1.867	7.627	0.020	0.021	7.64
						6.86
						7.54
	42.0					13.6
						14.4
						13.8
	50.2					29.6
						30.1
						29.3
	58.2					49.9
						49.9
						51.8
0.51	33.4	11.66	1.264	0.020	0.021	1.26
						1.68
						1.33
	42.0					3.00
						2.73
						2.77
	50.2					3.65
						4.75
						4.50
	58.2					8.93
						9.00
						7.60

Table S21. The mole fraction of [bmim][BF_4] **8**, the temperature, the exact amounts of ionic liquid **8**, methanol, the galactose **1**, and triethylamine, and the first order rate constant (k_1) for the process.

χ_8	Temp / °C	Mass ionic liquid / g	Mass MeOH / g	Mass galactose **1** / g	Mass NEt_3 / g	k_1 / 10^{-4} s^{-1}
0.02	33.4	1.711	7.541	0.021	0.020	6.28
						5.11
						5.22
	42.0					12.2
						11.0
						11.8
	50.2					25.4
						22.5
						24.0
	58.2					49.3
						44.0
						49.0
0.48	33.4	4.966	0.752	0.011	0.012	2.01
						1.48
						1.86
	42.0					3.61
						3.03
						3.56
	50.2	1.972	0.308	0.004	0.004	7.46
						6.38
						7.30
	58.2	1.976	0.307	0.004	0.006	13.9
						13.1
						12.2

Table S22. The mole fraction of [bmim][$C(CN)_3$] **9**, the temperature, the exact amounts of ionic liquid **9**, methanol, the galactose **1**, and triethylamine, and the first order rate constant (k_1) for the process.

χ_9	Temp / °C	Mass ionic liquid / g	Mass MeOH / g	Mass galactose **1** / g	Mass NEt_3 / g	k_1 / 10^{-4} s^{-1}
0.02	33.4	1.288	7.749	0.021	0.022	4.42
						5.08
						4.64
	42.0					11.2
						10.5
						10.2
	50.2					23.7
						23.1
						24.6
	58.2					42.3
						49.9
						45.0
0.50	33.4	4.453	0.629	0.011	0.011	0.89
						0.93
						0.94
	50.2					5.25
						4.56
						4.25
	58.2					9.66
						10.8
						8.99

^{1}H NMR spectra of synthesised compounds

All compounds were characterised using a Bruker Avance III 400 spectrometer. Spectra were processed using the Bruker Topspin 4.0.6 software.

1-Butyl-3-methylimidazolium bromide

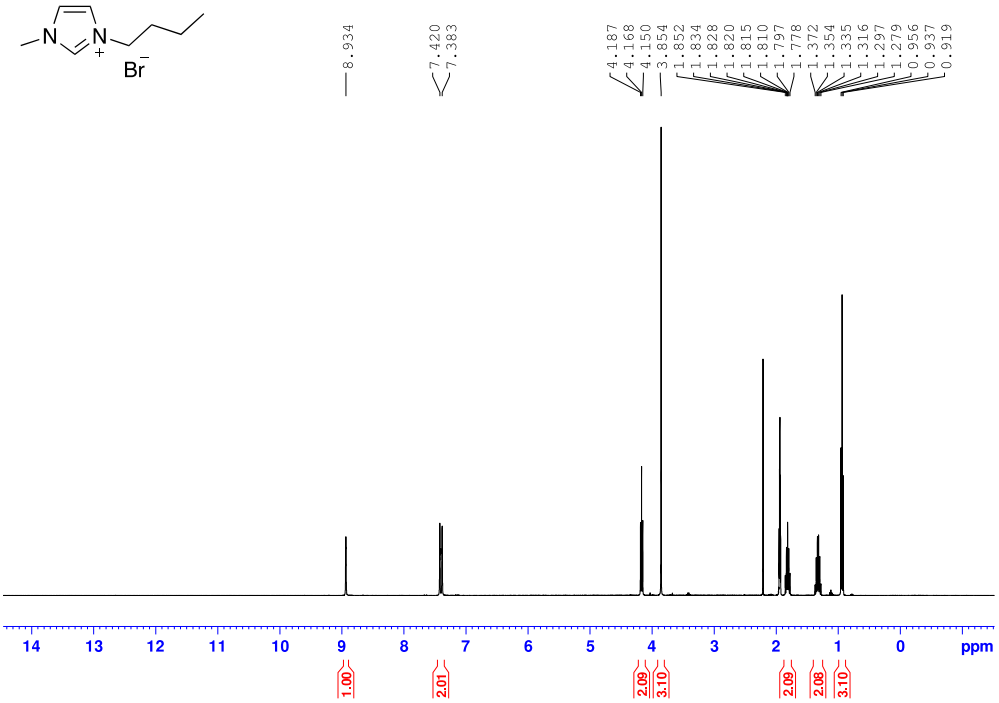

1-Butyl-2,3-dimethylimidazolium chloride

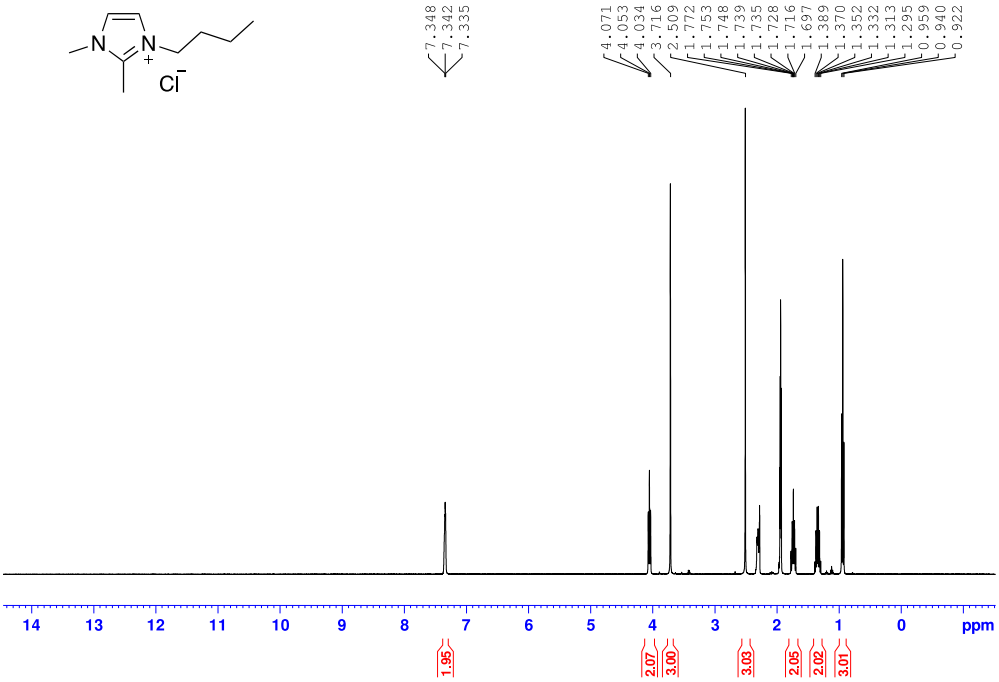

N-Butyl-*n*-methylpyrrolidinium bromide

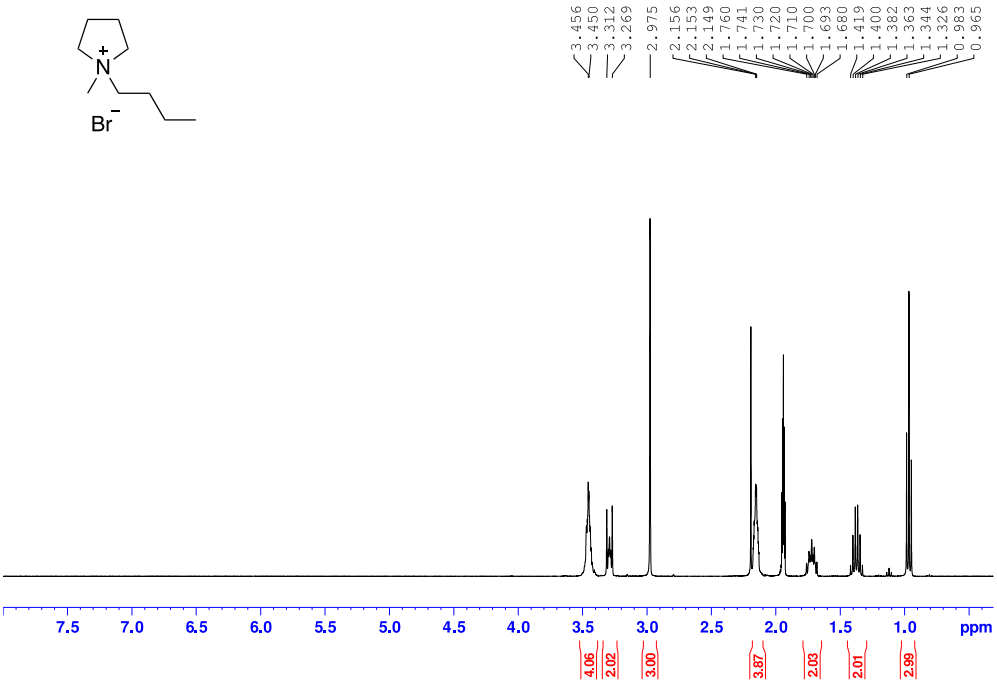

1-Butyl-3-methylimidazolium chloride

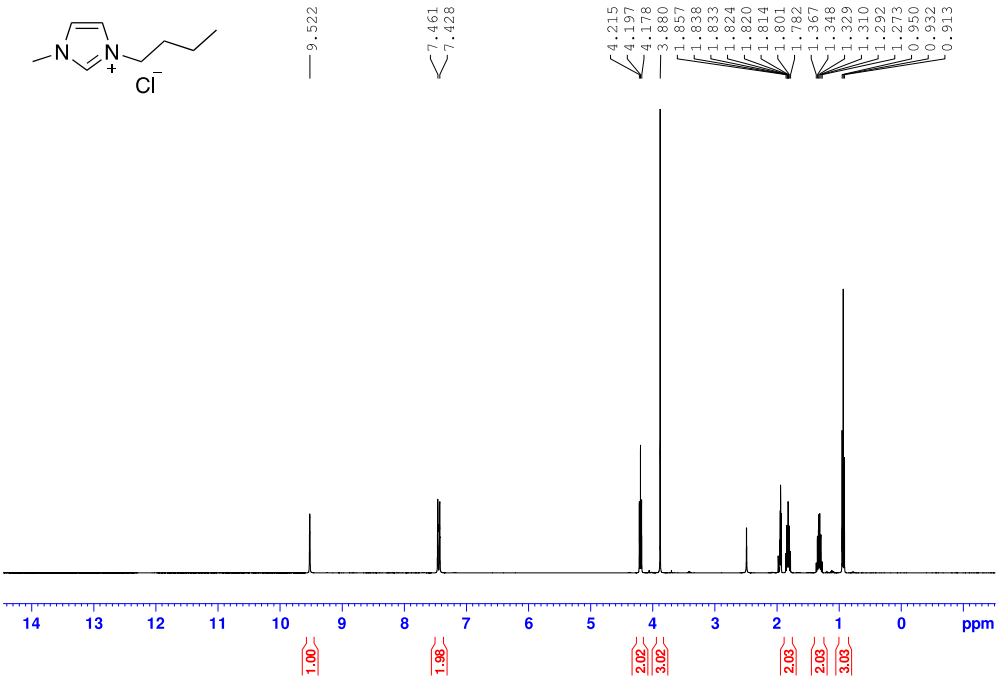

1-Butyl-3-methylimidazolium *bis*(trifluoromethanesulfonyl)imide **3**

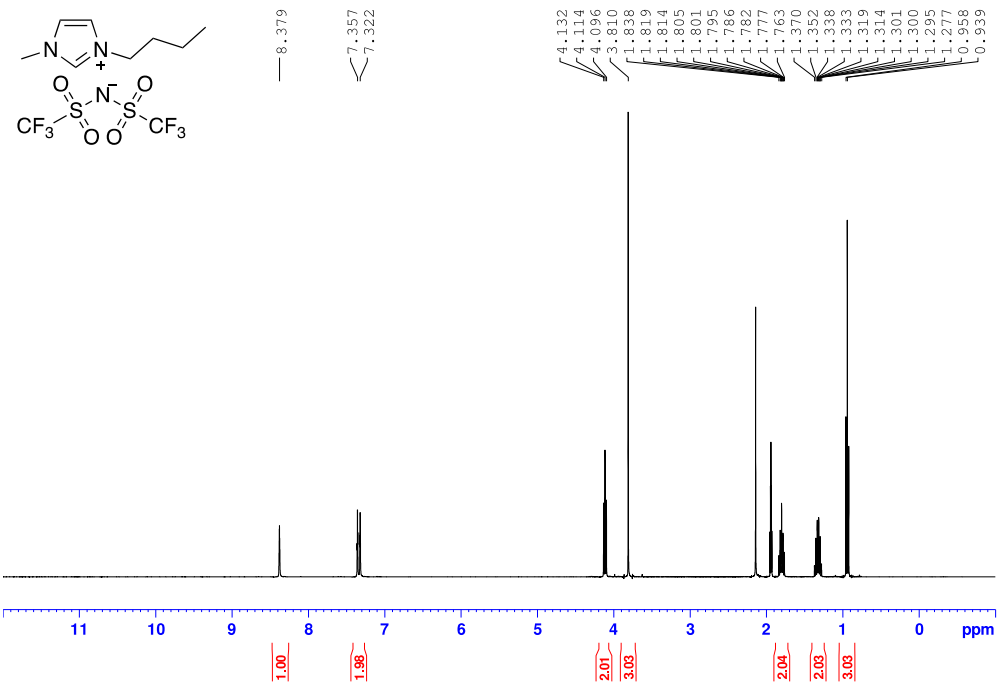

1-Butyl-2,3-dimethylimidazolium *bis*(trifluoromethanesulfonyl)imide **4**

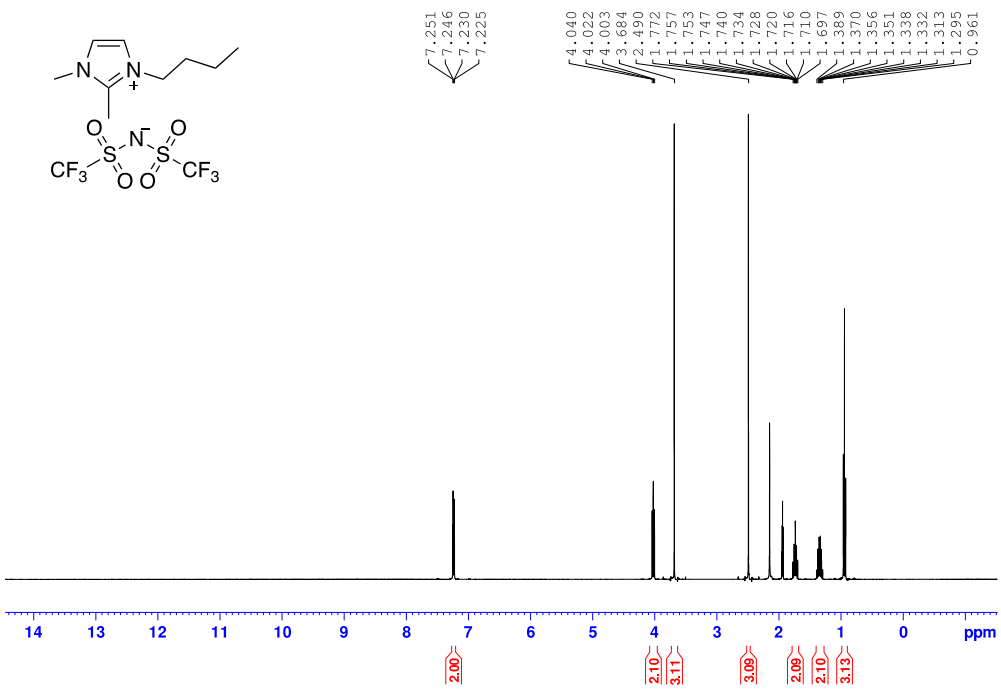

N-butyl-*n*-methylpyrrolidinium *bis*(trifluoromethanesulfonyl)imide **5**

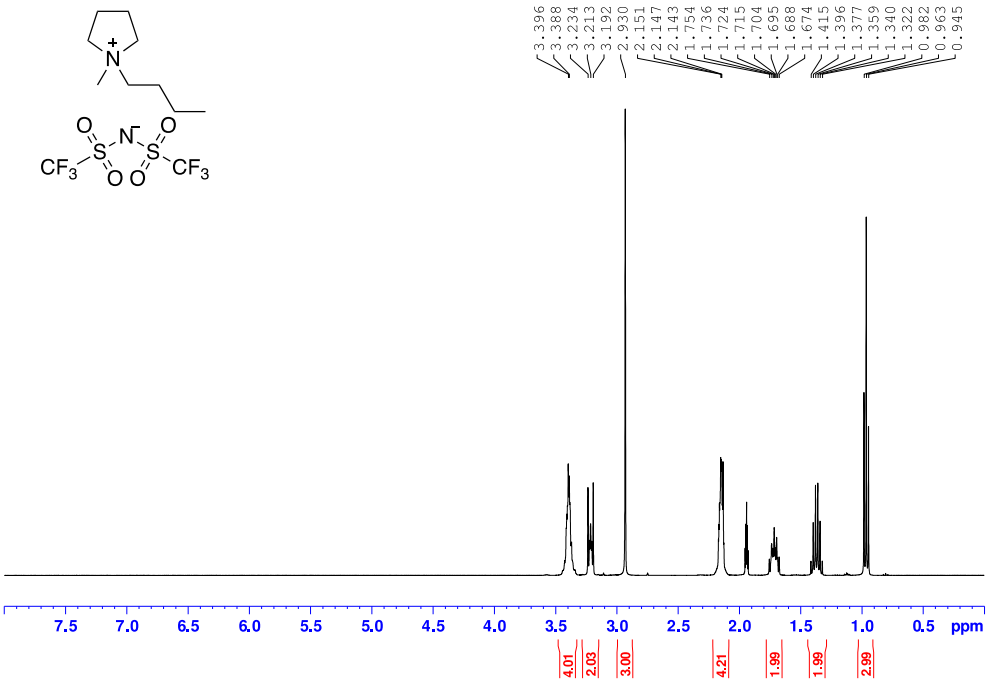

Methyltrioctylammonium *bis*(trifluoromethanesulfonyl)imide **6**

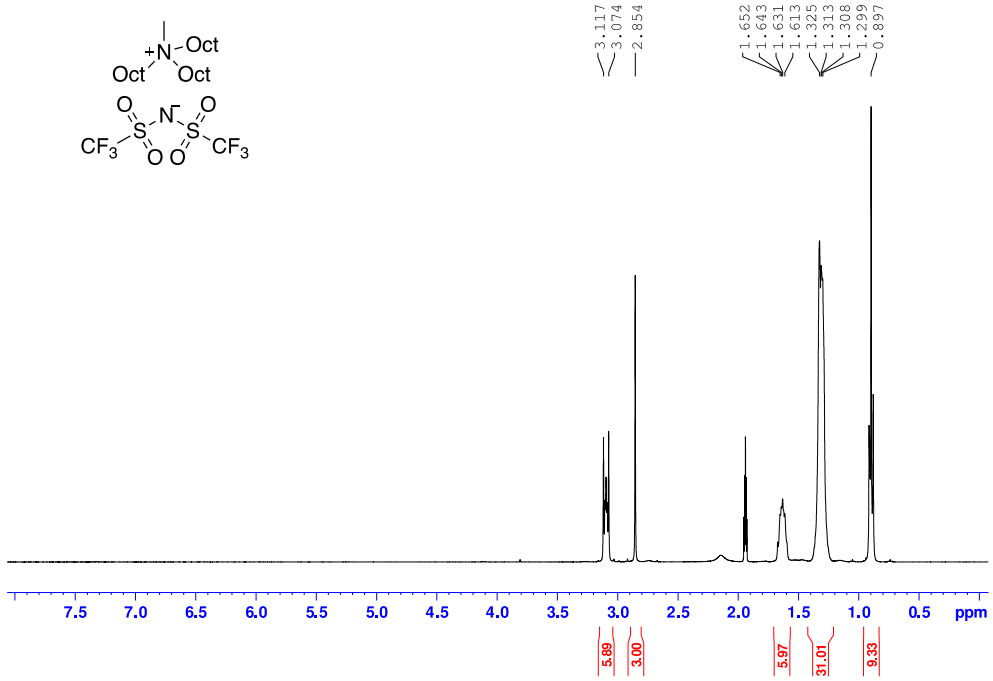

1-Butyl-3-methylimidazolium hexafluorophosphate **7**

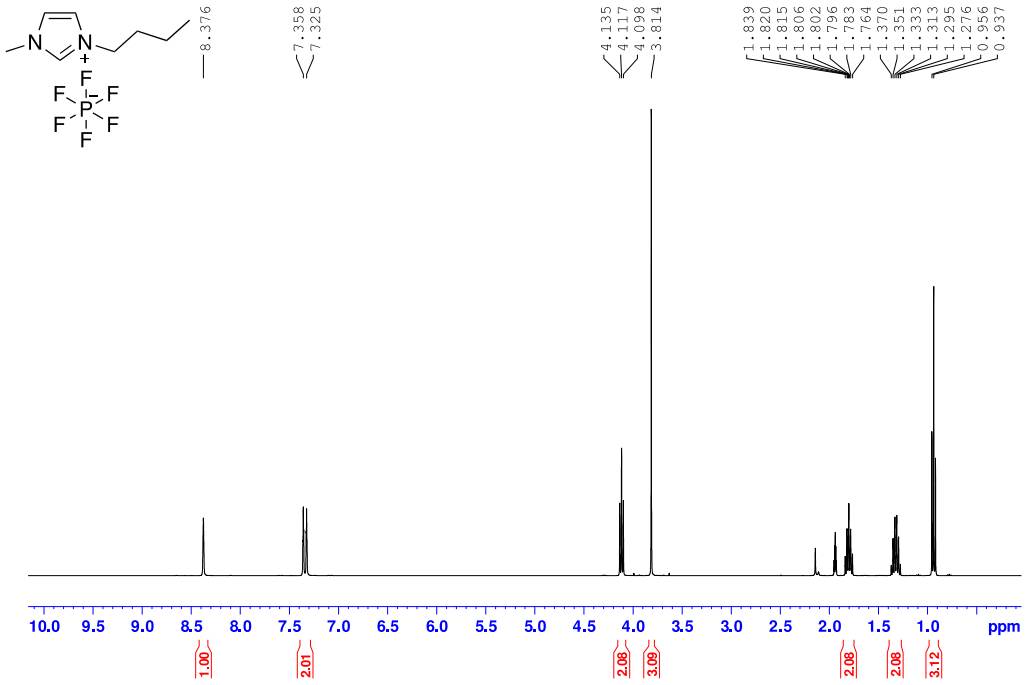

1-Butyl-3-methylimidazolium tetrafluoroborate **8**

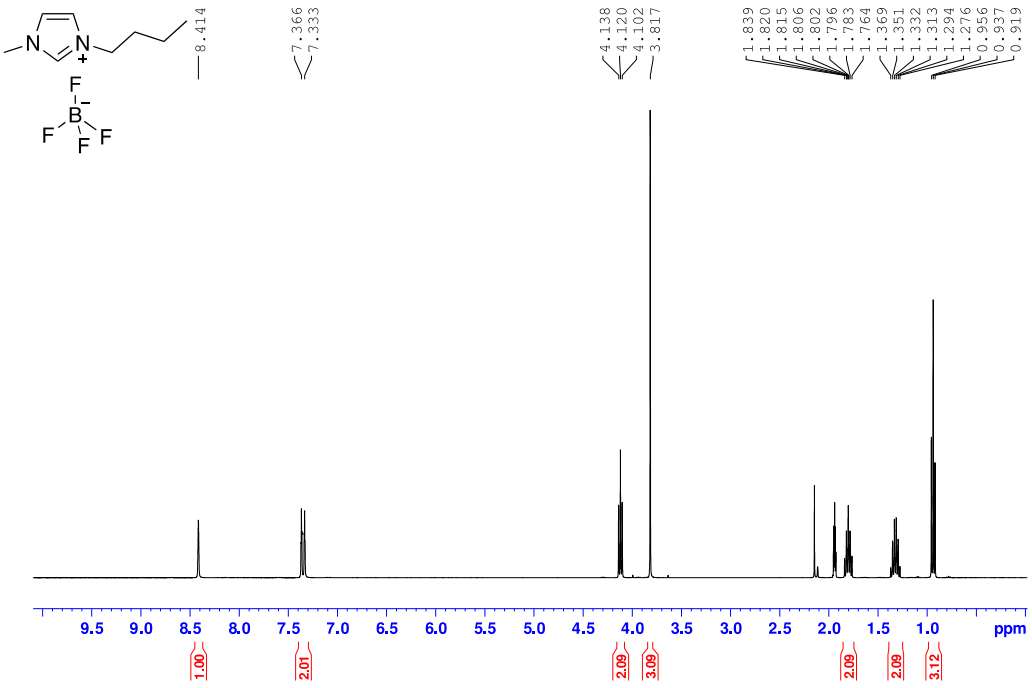

1-Butyl-3-methylimidazolium tricyanomethanide **9**

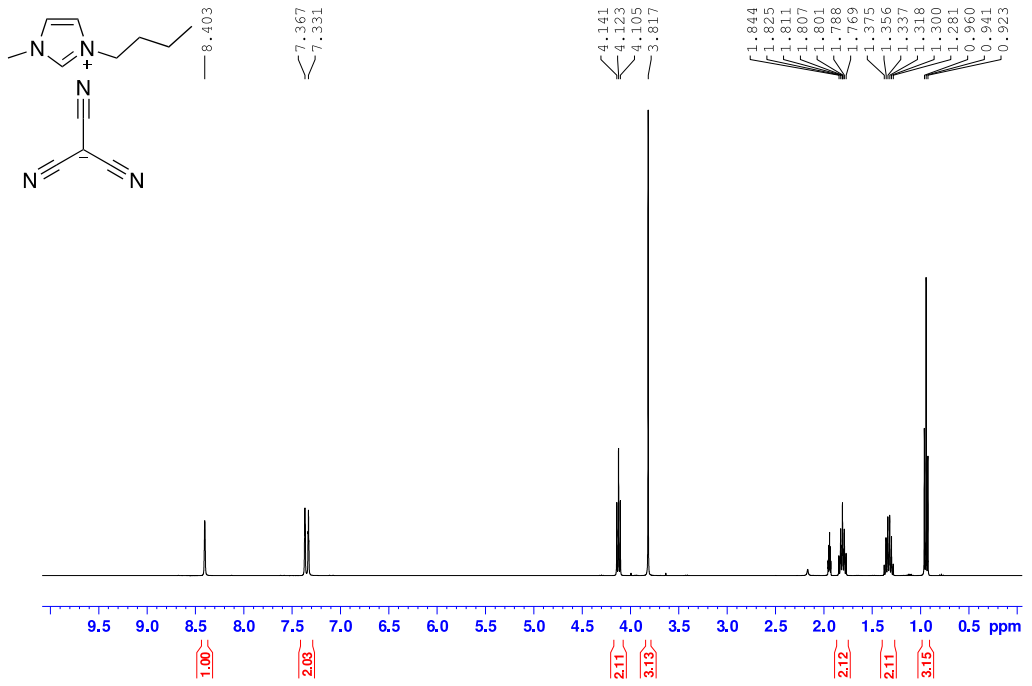

References

1. S. N. Baker, E. B. Brauns, T. M. McCleskey, A. K. Burrell and G. A. Baker, *Chem. Commun.*, 2006, 2851-2853.
2. A. Berthod, J. J. Kozak, J. L. Anderson, J. Ding and D. W. Armstrong, *Theor. Chem. Acc.*, 2007, **117**, 127-135.
3. L. Cammarata, S. G. Kazarian, P. A. Salter and T. Welton, *Phys. Chem. Chem. Phys.*, 2001, **3**, 5192-5200.
4. J. Zhu, L. Bai, B. Chen and W. Fei, *Chem. Eng. J.*, 2009, **147**, 58-62.
5. E. E. L. Tanner, R. R. Hawker, H. M. Yau, A. K. Croft and J. B. Harper, *Org. Biomol. Chem.*, 2013, **11**, 7516-7521.
6. V. Strehmel and V. Senkowski, *J. Polym. Sci. A*, 2015, **53**, 2849-2859.
7. J. Flieger and A. Czajkowska-Żelazko, *J. Sep. Sci.*, 2012, **35**, 248-255.
8. H. Srour, H. Rouault, C. C. Santini and Y. Chauvin, *Green Chem.*, 2013, **15**, 1341-1347.
9. G. Chatel, C. Monnier, N. Kardos, C. Voiron, B. Andrioletti and M. Draye, *Appl. Cat. A.*, 2014, **478**, 157-164.
10. I. S. Molchan, G. E. Thompson, R. Lindsay, P. Skeldon, V. Likodimos, G. E. Romanos, P. Falaras, G. Adamova, B. Iliev and T. J. S. Schubert, *RSC Adv.*, 2014, **4**, 5300-5311.
11. H. Eyring, *J. Chem. Phys.*, 1935, **3**, 107-115.
12. M. A. Ab Rani, A. Brant, L. Crowhurst, A. Dolan, M. Lui, N. H. Hassan, J. P. Hallett, P. A. Hunt, H. Niedermeyer, J. M. Perez-Arlandis, M. Schrems, T. Welton and R. Wilding, *Phys. Chem. Chem. Phys.*, 2011, **13**, 16831-16840.
13. Y. Dong, T. Takeshita, H. Miyafuji, T. Nokami and T. Itoh, *Bull. Chem. Soc. Jpn.*, 2018, **91**, 398-404.
14. R. Rinaldi, *Chem. Commun.*, 2011, **47**, 511-513.
15. D. Yalcin, A. J. Christofferson, C. J. Drummond and T. L. Greaves, *Phys. Chem. Chem. Phys.*, 2020, DOI: 10.1039/D0CP00201A.
16. R. Wang, J.-Z. Chen, X.-A. Zheng, R. Kong, S.-S. Gong and Q. Sun, *Carbohydr. Res.*, 2018, **455**, 114-118.
17. Ł. Szeleszczuk, T. Gubica, A. Zimniak, D. M. Pisklak, K. Dąbrowska, M. K. Cyrański and M. Kańska, *Chem. Phys. Lett.*, 2017, **686**, 7-11.
18. C.-W. Li, K.-W. Hon, B. Ghosh, P.-H. Li, H.-Y. Lin, P.-H. Chan, C.-H. Lin, Y.-C. Chen and K.-K. T. Mong, *Chem. Asian J.*, 2014, **9**, 1786-1796.
19. M. Giordano and A. Iadonisi, *Eur. J. Org. Chem.*, 2013, **2013**, 125-131.